

PARTIAL CHORD DIAGRAMS AND MATRIX MODELS

JØRGEN ELLEGAARD ANDERSEN, HIROYUKI FUJI, MASAHIDE MANABE,
ROBERT C. PENNER, AND PIOTR SUŁKOWSKI

ABSTRACT. In this article, the enumeration of partial chord diagrams is discussed via matrix model techniques. In addition to the basic data such as the number of backbones and chords, we also consider the Euler characteristic, the backbone spectrum, the boundary point spectrum, and the boundary length spectrum. Furthermore, we consider the boundary length and point spectrum that unifies the last two types of spectra. We introduce matrix models that encode generating functions of partial chord diagrams filtered by each of these spectra. Using these matrix models, we derive partial differential equations – obtained independently by cut-and-join arguments in an earlier work – for the corresponding generating functions.

CONTENTS

1. Introduction	2
1.1. Motivation: RNA chains	6
1.2. Plan of the paper	8
2. Enumerating partial linear chord diagrams via matrix models	9
2.1. A matrix model enumerating partial chord diagrams	9
2.2. A matrix model for the enumeration of chord diagrams	15
2.3. The boundary length and point spectrum and the unified model	19
3. Cut-and-join equations via matrix models	21
3.1. The boundary point spectrum	23
3.2. The boundary length spectrum	25
3.3. The boundary length and point spectrum	26
4. Non-oriented analogues	29
4.1. Non-oriented analogues of the matrix models	29
4.2. Non-oriented analogues of cut-and-join equations	33
Appendix A. Proof of Proposition 4.7	37
Appendix B. Proof of Lemma 4.9	38
References	40

Acknowledgments: JEA and RCP is supported in part by the center of excellence grant “Center for Quantum Geometry of Moduli Spaces” from the Danish National Research Foundation (DNRF95). The research of HF is supported by the Grant-in-Aid for Research Activity Start-up [# 15H06453], Grant-in-Aid for Scientific Research(C) [# 26400079], and Grant-in-Aid for Scientific Research(B) [# 16H03927] from the Japan Ministry of Education, Culture, Sports, Science and Technology. The work of MM and PS is supported by the ERC Starting Grant no. 335739 “Quantum fields and knot homologies” funded by the European Research Council under the European Union’s Seventh Framework Programme. PS also acknowledges the support of the Foundation for Polish Science, and RCP acknowledges the kind support of Institut Henri Poincaré where parts of this manuscript were written.

1. INTRODUCTION

A *partial chord diagram* is a special kind of graph, which is specified as follows. The graph consists of a number of line segments (which are called *backbones*) arranged along the real line (hence they come with an ordering), with a number of vertices on each. A number of semi-circles (called *chords*) arranged in the upper half plane is attached at a subset of the vertices of the line segments, in such a way that no two chords have endpoints at the same vertex. The vertices which are not attached to chord ends are called the marked points. A *chord diagram* is by definition a partial chord diagram with no marked points. Partial chord diagrams occur in many branches of mathematics, including topology [14, 30], geometry [9, 10, 3] and representation theory [16].

To each partial chord diagram c one can associate canonically a two dimensional surface with boundary Σ_c , see Figure 1. Moreover, as discussed in [56, 12, 2, 7], the notion of a *fatgraph* [42, 43, 44, 45] is a useful concept when studying partial chord diagrams. A fatgraph is a graph together with a cyclic ordering on each collection of half-edges incident on a common vertex. A partial linear chord diagram c has a natural fatgraph structure induced from its presentation in the plane.

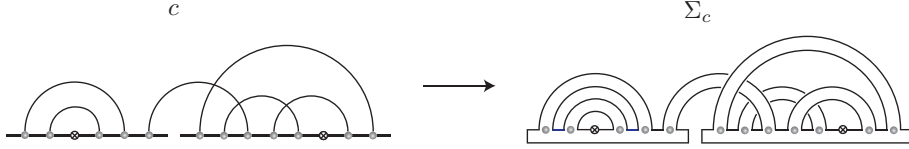


FIGURE 1. The partial chord diagram (with marked points) c and the corresponding surface Σ_c . The type of this partial chord diagram reads $\{g, k, l; \{b_i\}; \{n_i\}; \{p_i\}\} = \{1, 6, 2; \{b_6 = 1, b_8 = 1\}; \{n_0 = 2, n_1 = 2\}; \{p_1 = 1, p_2 = 2, p_9 = 1\}\}$. The boundary length and point spectrum is $\{n_{(1)} = 1, n_{(0,0)} = 2, n_{(0,0,0,0,0,1,0,0,0)} = 1\}$.

The partial chord diagram c is characterized by various topological data, and we will consider the following five types of data, introduced in [2] and [7].

- The number of chords k in c and the number of backbones b in c .
- Euler characteristic χ and genus g .
Let χ and g denote respectively the Euler characteristic and genus of Σ_c , which are related as follows

$$\chi = 2 - 2g.$$

Denoting by n the number of boundary components of Σ_c , the Euler relation can be written as

$$2 - 2g = b - k + n. \quad (1.1)$$

- Backbone spectrum (b_0, b_1, \dots) .
Let b_i denote the number of backbones with i trivalent (i.e. chord ends) or bivalent (i.e. marked points) vertices. The total number of backbones b is

then

$$b = \sum_{i \geq 0} b_i, \quad (1.2)$$

and the total number m of trivalent (i.e. chord ends) and bivalent (i.e. marked points) vertices of the partial chord diagram c is

$$m = \sum_{i \geq 1} i b_i. \quad (1.3)$$

- Boundary point spectrum (n_0, n_1, \dots) .

Let n_i denote the number of boundary components containing $i \geq 0$ marked points of Σ_c . The total number n of boundary components is

$$n = \sum_{i \geq 0} n_i, \quad (1.4)$$

and the total number l of marked points is

$$l = \sum_{i \geq 1} i n_i. \quad (1.5)$$

These three numbers m , k and l satisfies

$$m = 2k + l. \quad (1.6)$$

- Boundary length spectrum (p_1, p_2, \dots) .

Define the *length* of a boundary component to be the sum of the number of chords and the number of backbone undersides traversed by the boundary cycle. Let p_i be the number of boundary cycles with length $i \geq 1$. By definition, the following two relations hold

$$n = \sum_{i \geq 1} p_i, \quad (1.7)$$

$$2k + b = \sum_{i \geq 1} i p_i. \quad (1.8)$$

The data $\{g, k, l; \{b_i\}; \{n_i\}; \{p_i\}\}$ is called the *type* of a partial chord diagram c .

As a unification of the boundary length spectrum and the boundary point spectrum, we consider the *boundary length and point spectrum* introduced in [7]. Let us here recall its definition.

- Boundary length and point spectrum.

We associate a K -tuple of numbers $\mathbf{i} = (i_1, \dots, i_K)$ with a boundary component of length K , where i_L ($L = 1, \dots, K$) is the number of marked points between the L 'th and $(L + 1)$ 'th (taken modulo K) either chord or underpass of a backbone component (in either order) along the boundary.

Let $n_{\mathbf{i}}$ be the number of boundary components labeled in this way by \mathbf{i} . The total number l of marked points is

$$l = \sum_{K \geq 1} \sum_{\mathbf{i}} \sum_{L=1}^K i_L n_{(i_1, \dots, i_K)}, \quad (1.9)$$

and the total number n of boundary cycles is

$$n = \sum_{\mathbf{i}} n_{\mathbf{i}}. \quad (1.10)$$

The data $\{g, k, l; \{b_i\}, \{n_{\mathbf{i}}\}\}$ stores more detailed information on the distribution of marked points on each boundary component. One can determine the previous two kinds of spectra from the boundary length and point spectrum by forgetting the partitions of marked points on the boundary cycles.

It is known that the enumeration of chord diagrams is intimately related to matrix models and cut-and-join equations [4, 5, 6, 20, 38]. In this paper, the enumeration of partial chord diagrams labeled by the boundary length and point spectrum with the genus filtration is studied using matrix model techniques. Let $\mathcal{N}_{g,k,l}(\{b_i\}, \{n_{\mathbf{i}}\})$ denote the number of connected chord diagrams labeled by the set of parameters $(g, k, l; \{b_i\}; \{n_{\mathbf{i}}\})$. We define the generating function of these numbers

$$\begin{aligned} \mathcal{F}(x, y; \{s_i\}; \{u_{\mathbf{i}}\}) &= \sum_{b \geq 1} \mathcal{F}_b(x, y; \{s_i\}; \{u_{\mathbf{i}}\}), \\ \mathcal{F}_b(x, y; \{s_i\}; \{u_{\mathbf{i}}\}) &= \frac{1}{b!} \sum_{\sum_i b_i = b} \sum_{\{n_{\mathbf{i}}\}} \mathcal{N}_{g,k,l}(\{b_i\}, \{n_{\mathbf{i}}\}) x^{2g-2} y^k \prod_{i \geq 0} s_i^{b_i} \prod_{K \geq 1} \prod_{\{i_L\}_{L=1}^K} u_{\mathbf{i}}^{n_{\mathbf{i}}}. \end{aligned} \quad (1.11)$$

Generating functions of disconnected and connected diagrams are related via the exponential relation

$$\mathcal{Z}(x, y; \{s_i\}; \{u_{\mathbf{i}}\}) = \exp[\mathcal{F}(x, y; \{s_i\}; \{u_{\mathbf{i}}\})]. \quad (1.12)$$

To analyze this enumeration further, we write the above generating function as a certain Hermitian matrix integral. Let $\mathcal{Z}_N(y; \{s_i\}; \{u_{\mathbf{i}}\})$ be the matrix integral over rank N Hermitian matrices \mathcal{H}_N

$$\begin{aligned} \mathcal{Z}_N(y; \{s_i\}; \{u_{\mathbf{i}}\}) &= \\ &= \frac{1}{\text{Vol}_N} \int_{\mathcal{H}_N} dM \exp \left[-N \text{Tr} \left(\frac{M^2}{2} - \sum_{i \geq 0} s_i (y^{1/2} \Lambda_L^{-1} M + \Lambda_P)^i \Lambda_L^{-1} \right) \right], \end{aligned} \quad (1.13)$$

where Λ_P and Λ_L are *external matrices* [29] of rank N , and the normalization factor Vol_N is defined in (2.4). In this matrix integral representation, the counting parameter $u_{(i_1, \dots, i_K)}$ is identified with the trace of the corresponding product of external matrices

$$u_{(i_1, \dots, i_K)} = \frac{1}{N} \text{Tr} (\Lambda_P^{i_1} \Lambda_L^{-1} \Lambda_P^{i_2} \Lambda_L^{-1} \cdots \Lambda_P^{i_K} \Lambda_L^{-1}). \quad (1.14)$$

In Theorem 2.13 we show that

$$\mathcal{Z}_N(y; \{s_i\}; \{u_{\mathbf{i}}\}) = \mathcal{Z}(N^{-1}, y; \{s_i\}; \{u_{\mathbf{i}}\}). \quad (1.15)$$

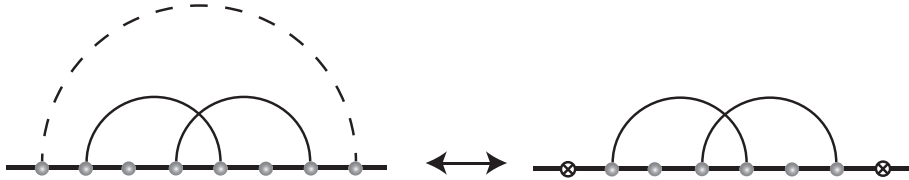


FIGURE 2. The cut-and-join manipulations on chord diagrams.

This matrix integral representation provides a new, matrix model proof of the cut-and-join equation found by combinatorial means in [7]. The cut-and-join equation can be written as

$$\frac{\partial}{\partial y} \mathcal{Z}(x, y; \{s_i\}; \{u_i\}) = \mathcal{M} \mathcal{Z}_N(x, y; \{s_i\}; \{u_i\}), \quad (1.16)$$

where \mathcal{M} is the second order partial differential operator in variables u_i (see Theorem 3.11 for details). This cut-and-join equation can be regarded as the evolution equation in the variable y , and its formal solution reads

$$\begin{aligned} \mathcal{Z}(x, y; \{s_i\}; \{u_i\}) &= e^{y\mathcal{M}} \mathcal{Z}(x, 0; \{s_i\}; \{u_i\}), \\ \mathcal{Z}(x, 0; \{s_i\}; \{u_i\}) &= e^{N^2 \sum_{i \geq 0} s_i u_{(i)}}. \end{aligned} \quad (1.17)$$

Expanding the operator $e^{y\mathcal{M}}$ around $y = 0$, one determines the number of connected partial chord diagrams $\mathcal{N}_{g,k,l}(\{b_i\}, \{n_i\})$ iteratively from this formal solution. The cut-and-join equation is a powerful method to systematically count partial chord diagrams of a given length and point spectrum.

In this work we also generalize the above analysis to non-oriented analogues of partial chord diagrams. By non-oriented partial chord diagrams we mean diagrams with all chords decorated by a binary variable, which indicates if they are *twisted* or not. When associating the surface Σ_c to a non-oriented partial chord diagram, twisted bands are associated along the twisted chords as indicated in Figure 3. This construction leads to 2^k orientable or non-orientable surfaces associated to one particular partial chord diagram with k chords, if we consider all possible assignments of twisting or untwisting of k bands. In the non-oriented case the Euler characteristic is defined as follows.

- Euler characteristic χ .

The Euler characteristic of the two dimensional surface Σ_c is defined by the formula

$$\chi = 2 - h,$$

where h is the number of cross-caps. The Euler relation holds

$$2 - h = b - k + n. \quad (1.18)$$

With this setup, the enumeration of non-oriented partial chord diagrams can be considered analogously to the orientable case.

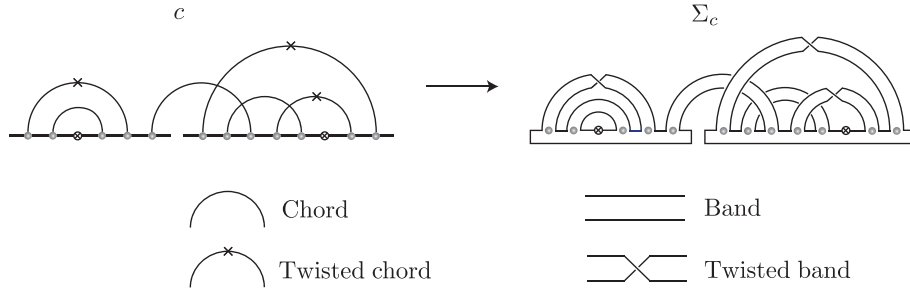


FIGURE 3. A non-oriented surface Σ_c associated to a non-oriented partial chord diagram c .

Let $\tilde{\mathcal{N}}_{h,k,l}(\{b_i\}, \{n_{\mathbf{i}}\})$ denote the number of connected non-oriented partial chord diagrams with the cross-cap number h , k chords, the backbone spectrum $\{b_i\}$, l marked points, and the boundary length and point spectrum $n_{\mathbf{i}}$. The generating function $\tilde{\mathcal{F}}(x, y; \{s_i\}; \{u_{\mathbf{i}}\})$ is defined by

$$\begin{aligned} \tilde{\mathcal{F}}(x, y; \{s_i\}; \{u_{\mathbf{i}}\}) &= \sum_{b \geq 1} \tilde{\mathcal{F}}_b(x, y; \{s_i\}; \{u_{\mathbf{i}}\}), \\ \tilde{\mathcal{F}}_b(x, y; \{s_i\}; \{u_{\mathbf{i}}\}) &= \frac{1}{b!} \sum_{\sum_i b_i = b} \sum_{\{n_{\mathbf{i}}\}} \tilde{\mathcal{N}}_{h,k,l}(\{b_i\}, \{n_{\mathbf{i}}\}) x^{h-2} y^k \prod_{i \geq 0} s_i^{b_i} \prod_{K \geq 1} \prod_{\{i_L\}_{L=1}^K} u_{\mathbf{i}}^{n_{\mathbf{i}}}. \end{aligned} \quad (1.19)$$

We also define the generating function of the numbers of connected and disconnected non-oriented partial chord diagrams

$$\tilde{\mathcal{Z}}(x, y; \{s_i\}; \{u_{\mathbf{i}}\}) = \exp \left[\tilde{\mathcal{F}}(x, y; \{s_i\}; \{u_{\mathbf{i}}\}) \right]. \quad (1.20)$$

In Theorem 4.5 we show that this generating function can be expressed as a real symmetric matrix integral with two external symmetric matrices Ω_P and Ω_L

$$\tilde{\mathcal{Z}}(N^{-1}, y; \{s_i\}; \{u_{\mathbf{i}}\}) = \tilde{\mathcal{Z}}_N(y; \{s_i\}; \{u_{\mathbf{i}}\}), \quad (1.21)$$

$$\begin{aligned} \tilde{\mathcal{Z}}_N(y; \{s_i\}; \{u_{\mathbf{i}}\}) &= \\ &= \frac{1}{\text{Vol}_N(\mathbb{R})} \int_{\mathcal{H}_N(\mathbb{R})} dM \exp \left[-N \text{Tr} \left(\frac{M^2}{4} - \sum_{i \geq 0} s_i (y^{1/2} \Omega_L^{-1} M + \Omega_P)^i \Omega_L^{-1} \right) \right], \end{aligned} \quad (1.22)$$

where the normalization factor $\text{Vol}_N(\mathbb{R})$ is defined in (4.8), and $\mathcal{H}_N(\mathbb{R})$ is the space of real symmetric matrices of rank N . The parameter $u_{(i_1, \dots, i_K)}$ is identified with a trace of the external matrices via the formula

$$u_{(i_1, \dots, i_K)} = \frac{1}{N} \text{Tr} (\Omega_P^{i_1} \Omega_L^{-1} \Omega_P^{i_2} \Omega_L^{-1} \dots \Omega_P^{i_K} \Omega_L^{-1}). \quad (1.23)$$

Using this matrix integral representation of the generating function, one can again prove the cut-and-join equation, established independently by combinatorial arguments in [7]

$$\frac{\partial}{\partial y} \tilde{\mathcal{Z}}_N(y; \{s_i\}; \{u_{\mathbf{i}}\}) = \tilde{\mathcal{M}} \tilde{\mathcal{Z}}_N(y; \{s_i\}; \{u_{\mathbf{i}}\}), \quad (1.24)$$

where $\tilde{\mathcal{M}}$ is a second order partial differential operator in the variables $u_{\mathbf{i}}$. The details of the differential operator $\tilde{\mathcal{M}}$ and the matrix model derivation of the cut-and-join equation are presented in Theorem 4.10.

1.1. Motivation: RNA chains. One important motivation to study partial chord diagrams in this and the preceding work [2, 7] is a complicated problem of RNA structure prediction in molecular biology, which we now shortly review.

An RNA molecule is a linear polymer, referred to as the backbone, that consists of four types of nucleotides: adenine, cytosine, guanine, and uracil, denoted respectively **A**, **C**, **G**, and **U**. The backbone is endowed with an orientation from 5'-end to 3'-end, and the primary sequence is the sequence of nucleotides read with respect to this orientation. Between nucleotides hydrogen bonds are formed, resulting in the so-called Watson-Click pairs involving **A** – **U** or **G** – **C** nucleotides; in addition Wobble pairs **U** – **G** can be formed. The set of base pairs formed by

such hydrogen bonds is referred to as the secondary structure.¹ Prediction of the secondary structure from the primary sequence is an outstanding problem that was initiated by the pioneering work of Michael Waterman [57] and has been studied intensively for last three decades.

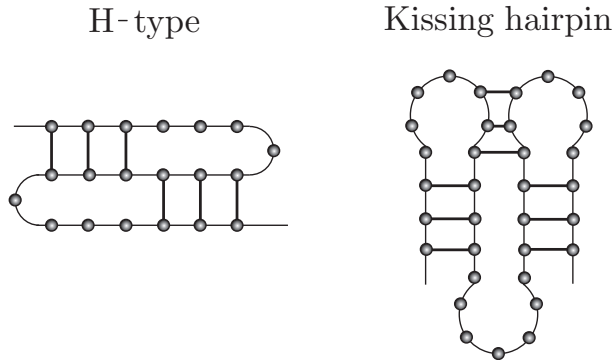


FIGURE 4. Pseudoknot structures in RNA. The long curved line, blobs (i.e. marked points), and short lines represent the backbone, nucleotides, and base pairs, respectively.

Topologically, we can represent the base pairings for a given RNA structure by a partial chord diagram as follows. The backbone is represented as a disjoint union of horizontal straight line segments (arranged along the real line in the plane), one for each backbone component, and each nucleotide is represented as a marked point on this union of line segments. The base pairs are represented by chords in the upper-half plane attached at two marked points corresponding to the bonded pair of nucleotides.

Note that a partial chord diagram has genus zero if no two of its chords cross each other. If however such crossings exist, then the structure is referred to as a pseudoknot, and its genus is non-zero. Considerable number of pseudoknot structures have been observed, e.g. tRNAs, RNaseP [31], telomerase RNA [53] and ribosomal RNAs [28]. According to the online database “RNA-strand” half of the known structures form pseudoknots [13]. There are various kinds of pseudoknots classified by the topology of the RNA [12], referred to as e.g. H-type [1], kissing hairpin [17, 51], etc.

In recent years, a combinatorial description of RNA structures in terms of linear chord diagrams has been developed in a series of works [41, 56, 55, 12, 11, 8, 4, 5, 2, 49, 46]. However, a large class of reasonable energy-based models that predict the secondary structure including pseudoknots are NP complete [32, 1], and a fully satisfactory energy model for RNA, including pseudoknot structures, has not been established yet.

In the search of a realistic energy function for RNA structures with pseudoknots, the boundary length and point spectrum should provide a useful tool that includes more detailed information about the location of marked points. In standard algorithms developed by Waterman [58], Nussinov et al. [40], Zucker and Stiegler

¹There are other types of interactions in RNA secondary structure, which are however less common and we ignore them in this discussion.

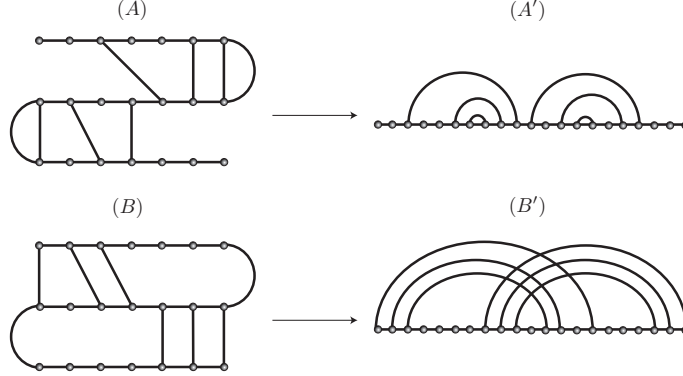


FIGURE 5. Partial chord diagrams unveil the difference in the topological structure of RNA molecules.

[61], etc., dynamic programming (DP) has been used to predict most likely secondary structures. Indeed, in famous algorithms such as [60, 25], the (loop-based) energy in each configuration of RNA is considered. In these algorithms, the most probable secondary structure is determined as the minimum free energy configuration, and to make them more efficient the statistical mechanical ensemble (i.e. the partition function algorithm) is implemented [34]. The application of these algorithms, which include pseudoknot structures stratified by γ structures, was studied in [50, 49]. Most of the energy functions essentially respect the boundary point and length spectra independently. In order to improve the energy model for RNA structure prediction with pseudoknots, it would be useful to explore energy parameters for more realistic and efficient energy function on the basis of the boundary length and point spectrum.

1.2. Plan of the paper. This paper is organized as follows. In Section 2 we construct Hermitian matrix models with external matrices, which encode generating functions of orientable partial chord diagrams labeled by the boundary point spectrum (in Subsection 2.1), the boundary length spectrum (in Subsection 2.2), and the boundary length and point spectrum (in Subsection 2.3). All these constructions are established by the correspondence between chord diagrams and Wick contractions via the Wick theorem. The matrix model encoding the boundary length and point spectrum is given in Theorem 2.13. In Section 3 we derive partial differential equations for matrix integrals found in Section 2. These partial differential equations coincide with the cut-and-join equations found combinatorially in [2, 7]. The cut-and-join equation for partial chord diagrams labeled by the boundary length and point spectrum is determined in Theorem 3.11. Section 4 is devoted to the analysis of non-oriented analogues of the results obtained in Section 2 and 3. In Subsection 4.1 we find real symmetric matrix models with external matrices, that encode generating functions of both orientable and non-orientable partial chord diagrams. The non-oriented analogue of the matrix integral from Theorem 2.13 is given in Theorem 4.5. Non-oriented analogues of cut-and-join equations from Section 3 are determined in Theorem 4.10. In Appendix A we derive a partial differential equation from Proposition 4.7 for a real symmetric matrix integral with external matrices. In Appendix B we prove Lemma 4.9.

2. ENUMERATING PARTIAL LINEAR CHORD DIAGRAMS VIA MATRIX MODELS

The enumeration problem of partial chord diagrams with respect to the genus filtration has been reformulated in terms of matrix integrals. Matrix model techniques for enumeration of the RNA structures with pseudoknots have been developed in a series of papers [41, 56, 55], and independently in [4, 5, 6]. Subsequently the analysis involving boundary point and length spectra of partial linear chord diagrams has been conducted in [2, 7]. In this section we develop a new perspective on this problem and construct a matrix model that enumerates partial chord diagrams labeled by the boundary length and point spectrum.

2.1. A matrix model enumerating partial chord diagrams. In the first step we construct a matrix model that counts partial chord diagrams labeled by the boundary point spectrum $\{n_i\}$.

Definition 2.1. Let $\mathcal{N}_{g,k,l}(\{b_i\}, \{n_i\}, \{p_i\})$ denote the number of connected partial chord diagrams of type $\{g, k, l; \{b_i\}; \{n_i\}; \{p_i\}\}$. In particular, focusing on the boundary point spectrum we define the following number of partial chord diagrams characterized by the data $\{g, k, l; \{b_i\}, \{n_i\}\}$,

$$\mathcal{N}_{g,k,l}(\{b_i\}, \{n_i\}) = \sum_{\{p_i\}} \mathcal{N}_{g,k,l}(\{b_i\}, \{n_i\}, \{p_i\}).$$

We introduce the generating function² for the numbers $\mathcal{N}_{g,k,l}(\{b_i\}, \{n_i\})$

$$\begin{aligned} F(x, y; \{s_i\}; \{t_i\}) &= \sum_{b \geq 1} F_b(x, y; \{s_i\}; \{t_i\}), \\ F_b(x, y; \{s_i\}; \{t_i\}) &= \frac{1}{b!} \sum_{\sum_i b_i = b} \sum_{\{n_i\}} \mathcal{N}_{g,k,l}(\{b_i\}, \{n_i\}) x^{2g-2} y^k \prod_{i \geq 0} s_i^{b_i} t_i^{n_i}. \end{aligned} \quad (2.1)$$

The generating function for the numbers $\hat{\mathcal{N}}_{k,b,l}(\{b_i\}, \{n_i\})$ of connected and disconnected partial chord diagrams arises in the usual way from the exponent

$$\begin{aligned} Z^P(x, y; \{s_i\}; \{t_i\}) &= \exp[F(x, y; \{s_i\}; \{t_i\})] \\ &= \sum_{\{b_i\}} \sum_{\{n_i\}} \hat{\mathcal{N}}_{k,b,l}(\{b_i\}, \{n_i\}) x^{-b+k-n} y^k \prod_{i \geq 0} s_i^{b_i} t_i^{n_i}. \end{aligned} \quad (2.2)$$

In the following we rewrite the generating function $Z^P(x, y; \{s_i\}; \{t_i\})$ as a Hermitian matrix integral. To this end, we consider first Gaussian averages over Hermitian matrices.

Definition 2.2. Let $\mathcal{O}(M)$ be a function of a rank N Hermitian matrix M . The Gaussian average $\langle \mathcal{O}(M) \rangle_N^G$ is defined by the integral over the space \mathcal{H}_N of rank N Hermitian matrices with respect to the Haar measure dM with the Gaussian weight $e^{-N \text{Tr} \frac{M^2}{2}}$,

$$\langle \mathcal{O}(M) \rangle_N^G = \frac{1}{\text{Vol}_N} \int_{\mathcal{H}_N} dM \mathcal{O}(M) e^{-N \text{Tr} \frac{M^2}{2}}, \quad (2.3)$$

where the normalization factor Vol_N takes form

$$\text{Vol}_N = \int_{\mathcal{H}_N} dM e^{-N \text{Tr} \frac{M^2}{2}} = N^{N(N+1)/2} \text{Vol}(\mathcal{H}_N). \quad (2.4)$$

² The parameters s_i and t_i in this article and in [2] are related by $s_i \leftrightarrow t_i$.

In particular for $\mathcal{O}(M) = M_{\alpha\beta}M_{\gamma\epsilon}$ ($\alpha, \beta, \gamma, \epsilon = 1, \dots, N$), the Gaussian average is

$$\overline{M_{\alpha\beta}M_{\gamma\delta}} := \langle M_{\alpha\beta}M_{\gamma\epsilon} \rangle_N^G = \frac{1}{N} \delta_{\alpha\epsilon} \delta_{\beta\gamma}. \quad (2.5)$$

This quantity is called the *Wick contraction*. By definition, a multiple Wick contraction is a product of the Gaussian average of each Wick contracted pair.

It follows from the definition (2.3) that Gaussian averages of an odd number of matrix elements vanish. On the other hand, Gaussian averages of an even number of matrix elements are non-zero, and can be computed using the *Wick theorem* [15, 43, 37], as we now recall. Consider an ordered sequence

$$M_{\alpha_1\beta_1}M_{\alpha_2\beta_2} \cdots M_{\alpha_{2k}\beta_{2k}}$$

of $2k$ matrix elements $M_{\alpha_n\beta_n}$ ($n = 1, \dots, 2k$).

Let P_k denote a set of matchings by k Wick contractions among the $2k$ matrix elements in the above sequence. P_k is isomorphic to the following quotient of groups

$$P_k \simeq G_H/G_E, \quad G_H = S_{2k}, \quad G_E = S_k \rtimes (S_2)^k.$$

Here the elements of the permutation group S_{2k} permute $2k$ matrix elements. The factors S_k of G_E act by permuting k Wick contractions and $(S_2)^k$ swaps matrix elements in each Wick contracted pair. The Wick theorem implies the following result.

Theorem 2.3. *The Gaussian average of $2k$ matrix elements $M_{\alpha_n\beta_n}$ ($n = 1, \dots, k$) equals*

$$\begin{aligned} \langle M_{\alpha_1\beta_1}M_{\alpha_2\beta_2} \cdots M_{\alpha_{2k}\beta_{2k}} \rangle_N^G &= \sum_{\sigma \in P_k} \prod_{i=1}^k \overline{M_{\alpha_{\sigma(2i-1)}\beta_{\sigma(2i-1)}} M_{\alpha_{\sigma(2i)}\beta_{\sigma(2i)}}} \\ &= \frac{1}{N^k} \sum_{\sigma \in P_k} \prod_{i=1}^k \delta_{\alpha_{\sigma(2i-1)}\beta_{\sigma(2i)}} \delta_{\alpha_{\sigma(2i)}\beta_{\sigma(2i-1)}}. \end{aligned} \quad (2.6)$$

2.1.1. Chord diagrams and Wick contractions. Let c be a chord diagram. We now recall the explicit relation between a surface Σ_c associated to a chord diagram c and k -matchings or Wick contractions in the Gaussian average. To illustrate this correspondence we depict chord ends on backbones in Σ_c as trivalent vertices that consist of upright and horizontal line segments, see Figure 6. This correspondence is specified by the following four points **C1**–**C4**.

- C1:** A matrix element $M_{\alpha\beta}$ corresponds to a chord end on a backbone. Indices $\alpha, \beta (= 1, \dots, N)$ are assigned to two upright line segments on the upper edge of the backbone.
- C2:** If two matrix elements $M_{\alpha_j\beta_j}M_{\alpha_{j+1}\beta_{j+1}}$ correspond to two adjacent chord ends on the same backbone, then the following quantity is assigned to the horizontal segment between these two chord ends on the upper edge of the backbone

$$\sum_{\alpha_{j+1}, \beta_j=1}^N \delta_{\beta_j\alpha_{j+1}}.$$

This assignment encodes matrix multiplication of matrix elements corresponding to adjacent chord ends on the backbone.

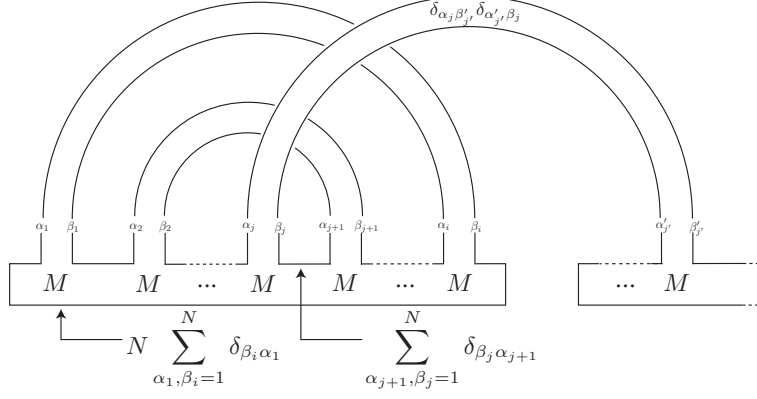


FIGURE 6. Bijective correspondence between chord diagrams and Wick contractions.

C3: For the product of i matrix elements M

$$\sum_{\alpha_2, \dots, \alpha_i=1}^N \sum_{\beta_1, \dots, \beta_{i-1}=1}^N M_{\alpha_1 \beta_1} \delta_{\beta_1 \alpha_2} M_{\alpha_2 \beta_2} \dots \delta_{\beta_{i-1} \alpha_i} M_{\alpha_i \beta_i} = (M^i)_{\alpha_1 \beta_i},$$

which corresponds to a backbone with i chord ends, the following quantity is assigned to the bottom edge of the backbone

$$N \sum_{\alpha_1, \beta_i=1}^N \delta_{\beta_i \alpha_1}.$$

Thus, a backbone with i chord ends corresponds to a single trace of the i 'th power of M , namely $N \text{Tr} M^i$.

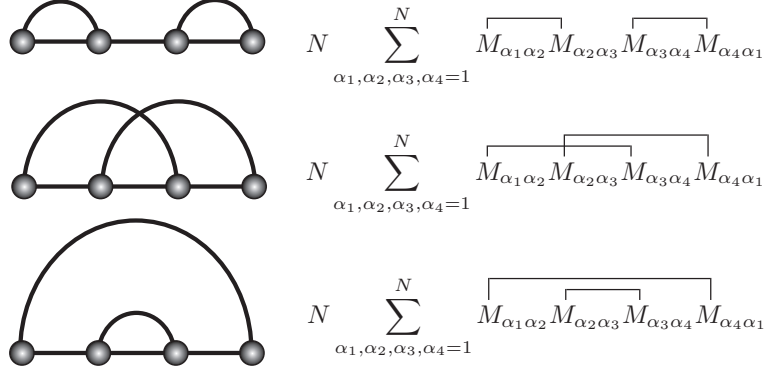
C4: The Wick contraction between $M_{\alpha_j \beta_j}$ and $M_{\alpha'_j \beta'_j}$ corresponds to a band connecting two chord ends. Each Wick contraction imposes a constraint $\delta_{\alpha_j \beta'_j} \delta_{\alpha'_j \beta_j}$ on matrix indices assigned to the edges of the chord ends matched by the Wick contraction.

The above rules imply the following bijective correspondence

$$W_N^C(\{b_i\}) = \left\langle \prod_i (N \text{Tr} M^i)^{b_i} \right\rangle_N^G, \quad \sum_i i b_i = 2k, \quad (2.7)$$

between matchings by k Wick contractions in the Gaussian average on one hand, and chord diagrams that consist of b_i backbones with i chord ends on the other hand, see Figure 7.

The Wick contractions (2.6) in $W_N^C(\{b_i\})$ replace all matrix elements M 's by products of δ 's, and summing over matrix indices along a boundary cycle one finds a factor of N corresponding to each boundary cycle in a chord diagram. Therefore the overall N dependence following from the above rules amounts to assigning N^{b-k+n} factor to the term $W_N^C(\{b_i\})$, corresponding to a chord diagram with backbone spectrum $\{b_i\}$ and n boundary cycles. Combining the Wick theorem and this bijective correspondence between matchings by k Wick contractions in the Gaussian average $W_N^C(\{b_i\})$ and the set of chord diagrams with backbone spectrum $\{b_i\}$, the following proposition follows.

FIGURE 7. Chord diagrams and Wick contractions for $\langle N \text{Tr} M^4 \rangle_N^G$.

Proposition 2.4. *The Gaussian average $W_N^C(\{b_i\})$ in equation (2.7) agrees with the generating function of chord diagrams with backbone spectrum $\{b_i\}$*

$$W_N^C(\{b_i\}) = \sum_{n \geq 0} \hat{\mathcal{N}}_{k,b,n}(\{b_i\}) N^{b-k+n}. \quad (2.8)$$

Here $\hat{\mathcal{N}}_{k,b,n}(\{b_i\})$ is the number of chord diagrams that consist of b_i backbones with i trivalent vertices

$$\hat{\mathcal{N}}_{k,b,n}(\{b_i\}) = \sum_{\{p_i\}} \hat{\mathcal{N}}_{k,b,l=0}(\{b_i\}, n_0 = n, \{n_i = 0\}_{i \geq 1}, \{p_i\}). \quad (2.9)$$

2.1.2. Partial chord diagrams and Wick contractions. We now generalize the above bijective correspondence to partial chord diagrams. Let c be a partial chord diagram. On the boundary cycles of the surface Σ_c we add additional marked points, which correspond to those marked points on c which are not chord ends. These marked points are represented by *external matrices* Λ_P of rank N in the Gaussian average. The rules **P1**–**P5** below provide the correspondence between partial chord diagrams with backbone spectrum $\{b_i\}$ and matchings with k Wick contractions in the Gaussian average.

P1: A matrix element $M_{\alpha\beta}$ corresponds to a chord end on a backbone. The graphical rule is the same as the rule **C1**.

P2: A matrix element $\Lambda_{P\alpha\beta}$ corresponds to a marked point on a backbone in Σ_c . Indices $\alpha, \beta (= 1, \dots, N)$ are assigned to two upright line segments at each marked point on the upper edge of the backbone, see Figure 8.

P3: To a line segment (on the upper edge of the backbone) between adjacent chord ends or marked points (located on the same backbone), corresponding to matrix elements $U_{\alpha_j \beta_j}$ and $V_{\alpha_{j+1} \beta_{j+1}}$ (for $U, V = M$ or Λ_P), we assign

$$\sum_{\beta_j, \alpha_{j+1}=1}^N \delta_{\beta_j \alpha_{j+1}}, \quad (2.10)$$

just as in **C2**.

P4: Let $v_j, w_j \in \mathbb{Z}_{\geq 0}$ ($j = 1, \dots, i$) with $\sum_{j=1}^i (v_j + w_j) = i$. For an ordered matrix product

$$(M^{v_1} \Lambda_P^{w_1} M^{v_2} \Lambda_P^{w_2} \dots M^{v_i} \Lambda_P^{w_i})_{\alpha_1 \beta_i}, \quad (2.11)$$

corresponding to a backbone which is an ordered sequence of v_j chord ends and w_j marked points, we assign

$$N \sum_{\alpha_1, \beta_i=1}^N \delta_{\beta_i \alpha_1}$$

to the bottom edge of this backbone. It follows that the trace

$$N \text{Tr}(M^{v_1} \Lambda_P^{w_1} M^{v_2} \Lambda_P^{w_2} \dots M^{v_i} \Lambda_P^{w_i}) \quad (2.12)$$

is assigned to this backbone.

P5: The Wick contraction between $M_{\alpha_j \beta_j}$ and $M_{\alpha'_{j'}, \beta'_{j'}}$ corresponds to a band connecting two chord ends, and it is represented in the same way as specified in **C4**.

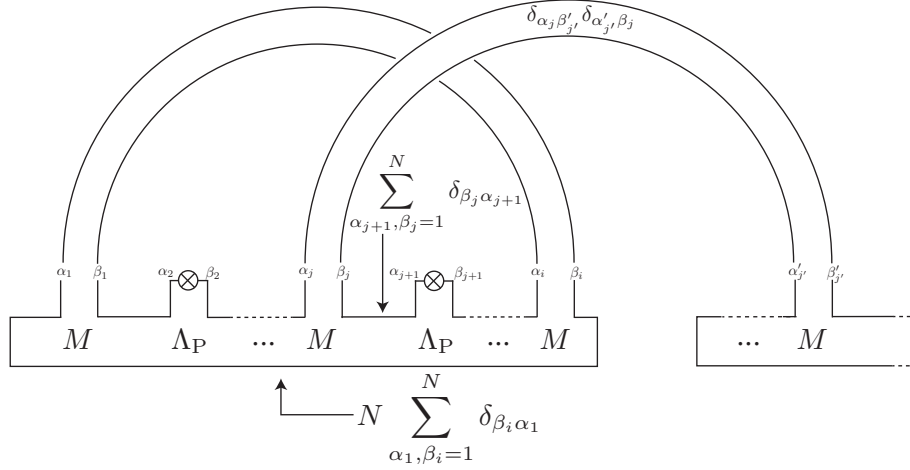


FIGURE 8. Bijective correspondence between partial chord diagrams and matchings of Wick contractions

For a fixed backbone spectrum $\{b_i\}$, all possible sequences $\{\alpha_j, \beta_j\}$ in the expression (2.12) are generated by the following product of traces

$$\prod_{i \geq 0} (N \text{Tr}(M + \Lambda_P)^i)^{b_i}. \quad (2.13)$$

Hence, by the above rules, all partial chord diagrams with the backbone spectrum $\{b_i\}$ correspond bijectively to all matchings by Wick contractions among the M 's in the expansion of the Gaussian average

$$W_N^P(\{b_i\}, \{r_i\}) = \left\langle \prod_{i \geq 0} (N \text{Tr}(M + \Lambda_P)^i)^{b_i} \right\rangle_N^G, \quad (2.14)$$

where we introduced the reverse Miwa times

$$r_i = \frac{1}{N} \text{Tr} \Lambda_P^i. \quad (2.15)$$

If there are n_i boundary components containing i marked points, then one finds a trace factor $(\text{Tr} \Lambda_P^i)^{n_i}$ in the corresponding term in the Gaussian average (2.14), see Figure 9. Therefore, for partial chord diagrams with the backbone spectrum $\{b_i\}$ and the boundary point spectrum $\{n_i\}$, the corresponding term in $W_N^P(\{b_i\}, \{r_i\})$ contributes the factor

$$N^{b-k+n} \prod_{i \geq 0} r_i^{n_i}.$$

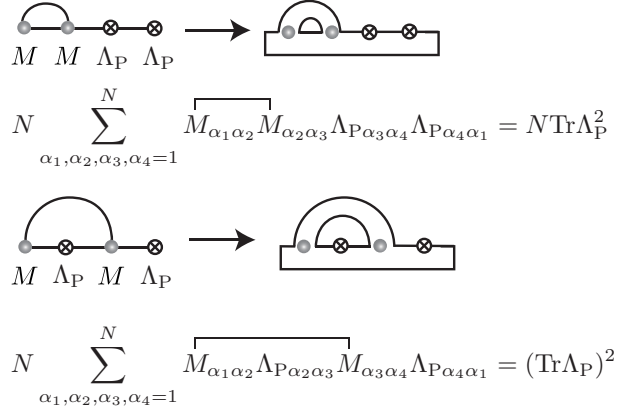


FIGURE 9. Partial chord diagrams of types $\{g = 0, k = 1, l = 2; b_4 = 1; n_0 = 1, n_2 = 1\}$ and $\{g = 0, k = 1, l = 2; b_4 = 1; n_1 = 2\}$, and the corresponding Wick contractions.

Therefore, from Wick theorem and the above bijective correspondence between partial chord diagrams and matchings by Wick contractions, one finds the following proposition.

Proposition 2.5. *The Gaussian average (2.14) is the generating function for the numbers $\hat{\mathcal{N}}_{k,b,l}(\{b_i\}, \{n_i\})$ of partial chord diagrams with the backbone spectrum $\{b_i\}$ and the boundary point spectrum $\{n_i\}$*

$$W_N^P(\{b_i\}, \{r_i\}) = \sum_{\{n_i\}} \hat{\mathcal{N}}_{k,b,l}(\{b_i\}, \{n_i\}) N^{b-k+n} \prod_{i \geq 0} r_i^{n_i}, \quad (2.16)$$

where the summation is constrained by $\sum i n_i = \sum i b_i - 2k$.

Using this proposition, we consider the full generating function $Z_N^P(y; \{s_i\}; \{r_i\})$ for the numbers $\hat{\mathcal{N}}_{k,b,l}(\{b_i\}, \{n_i\})$ of partial chord diagrams weighted by

$$N^{b-k+n} y^k \prod_{i \geq 0} s_i^{b_i} r_i^{n_i}.$$

Since the contribution from a partial chord diagram is invariant under permutations of its backbones, the full generating function

$$Z_N^P(y; \{s_i\}; \{r_i\}) = \sum_{\{b_i\}} \sum_{\{n_i\}} \hat{\mathcal{N}}_{k,b,l}(\{b_i\}, \{n_i\}) N^{b-k+n} y^k \prod_{i \geq 0} s_i^{b_i} r_i^{n_i}$$

can be rewritten as a sum over all backbone spectra $\{b_i\}$ of the terms

$$y^{\sum_i i b_i / 2} W_N^P(\{b_i\}, \{y^{-i/2} r_i\}) \prod_i \frac{s_i^{b_i}}{b_i!}.$$

It follows that

$$Z_N^P(y; \{s_i\}; \{r_i\}) = \sum_{\{b_i\}} \prod_{i \geq 0} \frac{s_i^{b_i} y^{i b_i / 2}}{b_i!} \left\langle \left(N \text{Tr}(M + y^{-1/2} \Lambda_P)^i \right)^{b_i} \right\rangle_N^G.$$

Performing the summation over b_i 's, one finds that the full generating function is given by the matrix integral

$$\begin{aligned} Z_N^P(y; \{s_i\}; \{r_i\}) &= \\ &= \frac{1}{\text{Vol}_N} \int_{\mathcal{H}_N} dM \exp \left[-N \text{Tr} \left(\frac{M^2}{2} - \sum_{i \geq 0} s_i (y^{1/2} M + \Lambda_P)^i \right) \right]. \end{aligned} \quad (2.17)$$

This matrix integral and $Z^P(x, y; \{s_i\}; \{t_i\})$ in equation (2.2) are identified by a change of variables. Since the reverse Miwa time for $i = 0$ yields $r_0 = 1$ automatically, we need to introduce the parameter t_0 by the following change of variables

$$N \rightarrow t_0 N, \quad y \rightarrow t_0 y, \quad s_i \rightarrow t_0^{-1} s_i, \quad r_i \rightarrow t_0^{-1} t_i.$$

As a result, we find the main theorem in this subsection.

Theorem 2.6. *The generating function (2.2) is given by the matrix integral (2.17),*

$$Z^P(N^{-1}, y; \{s_i\}; \{t_i\}) = Z_{t_0 N}^P(t_0 y; \{t_0^{-1} s_i\}; \{t_0^{-1} t_i\}). \quad (2.18)$$

2.2. A matrix model for the enumeration of chord diagrams. Next we turn to the enumeration of chord diagrams labeled by the backbone spectrum $\{b_i\}$ and the boundary length spectrum $\{p_i\}$. The number $\mathcal{N}_{g,k}(\{b_i\}, \{p_i\})$ of connected chord diagrams is given by

$$\mathcal{N}_{g,k}(\{b_i\}, \{p_i\}) = \sum_{\{n_i\}} \mathcal{N}_{g,k,0}(\{b_i\}, \{n_i\}, \{p_i\}).$$

We introduce the following generating function of these numbers³

Definition 2.7. Let $G(x, y; \{s_i\}; \{q_i\})$ denote the generating function of chord diagrams labeled by the boundary length spectrum

$$\begin{aligned} G(x, y; \{s_i\}; \{q_i\}) &= \sum_{b \geq 1} G_b(x, y; \{s_i\}; \{q_i\}), \\ G_b(x, y; \{s_i\}; \{q_i\}) &= \frac{1}{b!} \sum_{\sum b_i = b} \sum_{\{p_i\}} \mathcal{N}_{g,k}(\{b_i\}, \{p_i\}) x^{2g-2} y^k \prod_{i \geq 0} s_i^{b_i} \prod_{i \geq 1} q_i^{p_i}. \end{aligned} \quad (2.19)$$

³ The parameters q_i 's in our paper correspond to s_i 's in [2].

In the same way as the generating function $Z^P(x, y; \{s_i\}; \{t_i\})$ in (2.2), the generating function for the numbers $\hat{\mathcal{N}}_{k,b}(\{b_i\}, \{p_i\})$ of connected and disconnected chord takes form

$$\begin{aligned} Z^L(x, y; \{s_i\}; \{q_i\}) &= \exp[G(x, y; \{s_i\}; \{q_i\})] \\ &= \sum_{\{b_i\}} \sum_{\{p_i\}} \hat{\mathcal{N}}_{k,b}(\{b_i\}; \{p_i\}) x^{-b+k-n} y^k \prod_{i \geq 0} s_i^{b_i} \prod_{i \geq 1} q_i^{p_i}. \end{aligned} \quad (2.20)$$

2.2.1. A matrix model for the boundary length spectrum. Let c be a chord diagram. The boundary length spectrum filters chord diagrams according to combinatorial length of each boundary cycle, i.e. the sum of the number of chords and backbone underpasses. This length can be determined by counting marked points of a new type, which we now introduce. We introduce marked points of a new type between all chord ends and backbone ends, see the left diagram in Figure 10. For chord diagram decorated in this way, we get new marked points on the boundaries of the surface Σ_c by sliding each new marked point along the boundary of Σ_c until it reaches the first chord or backbone underside midpoint, as indicated in the right hand side of Figure 10.

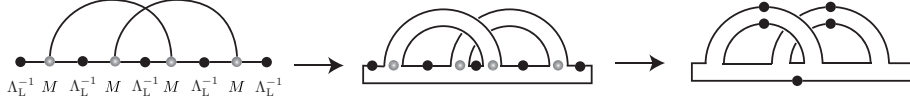


FIGURE 10. Decorating a chord diagram with new marked points for partitions.

In order to construct a Gaussian matrix integral which counts this type of chord diagrams we introduce another external matrix Λ_L , which is an invertible rank N matrix that keeps track of new marked points. We introduce a new model based on the following rules **L1**–**L5**, in which Wick contractions in the Gaussian average correspond bijectively to decorated chord diagrams.

- L1:** A matrix element $M_{\alpha\beta}$ corresponds to a chord end on a backbone. This graphical rule is the same as the rule **C1**.
- L2:** A matrix element $(\Lambda_L^{-1})_{\alpha_j\beta_j}$ is adjacent to a matrix element $M_{\alpha_{j+1}\beta_{j+1}}$ on an upper edge of a backbone in Σ_c . Without loss of generality, we can put Λ_L^{-1} 's on the left hand side of the M 's. Indices $\alpha_j, \beta_j (= 1, \dots, N)$ are assigned to two upright line segments nipping a marked point in the upper edge of the backbone, see Figure 11.
- L3:** If two matrix elements $U_{\alpha_j\beta_j}$ and $V_{\alpha_{j+1}\beta_{j+1}}$ ($U, V = M$ or Λ_L^{-1}) on the same backbone are adjacent, we form a matrix product $(UV)_{\alpha_j\beta_{j+1}}$. This graphical rule is the same as the rule **C2**.
- L4:** If a matrix product

$$(\Lambda_L^{-1} M)_{\alpha_1\beta_i}^i$$

corresponds to a backbone with a marked point, we assign the expression

$$N \sum_{\alpha_1, \beta_i=1}^N (\Lambda_L^{-1})_{\alpha_1\beta_i}$$

to the bottom edge of this backbone. This gives the contribution

$$N\text{Tr}((\Lambda_L^{-1}M)^i\Lambda_L^{-1})$$

with i chord ends and therefore $i + 1$ new marked points.

L5: The Wick contraction between $M_{\alpha_j\beta_j}$ and $M_{\alpha'_j\beta'_j}$ corresponds to a band connecting two chord ends. This graphical rule is the same as the rule **C4**.

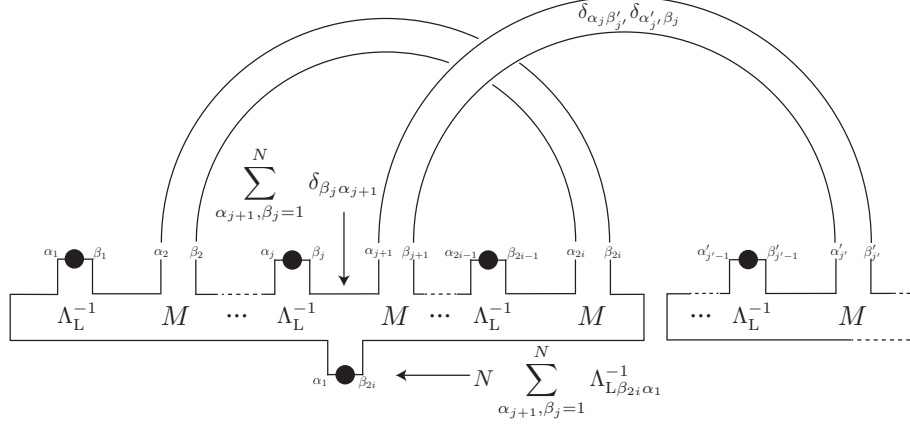


FIGURE 11. Bijective correspondence between decorated chord diagrams and matchings of Wick contractions.

Repeating the same discussions as in the previous subsection, one finds that every chord diagram with the backbone spectrum $\{b_i\}$ corresponds to matchings with $k = \sum ib_i/2$ Wick contractions, which arise from the following Gaussian average

$$W_N^L(\{b_i\}; \{q_i\}) = \left\langle \prod_{i \geq 0} (N\text{Tr}(\Lambda_L^{-1}M)^i \Lambda_L^{-1})^{b_i} \right\rangle_N^G, \quad (2.21)$$

where we introduced Miwa times

$$q_i = \frac{1}{N} \text{Tr} \Lambda_L^{-i}. \quad (2.22)$$

It follows from the rules **L1–L5** that i Λ_L^{-1} 's are aligned along the boundary cycle with length i . Therefore, for chord diagrams with the backbone spectrum $\{b_i\}$ and the boundary length spectrum $\{p_i\}$, the corresponding Wick contractions in $W_N^L(\{b_i\}; \{q_i\})$ involve the factor

$$N^{b-k+n} \prod_{i \geq 1} q_i^{p_i},$$

see Figure 12. The key proposition of this subsection follows.

Proposition 2.8. *The Gaussian average $W_N^L(\{b_i\}; \{q_i\})$ in eq.(2.21) is the generating function of the numbers $\hat{N}_{k,b}(\{b_i\}, \{p_i\})$ of chord diagrams with the backbone spectrum $\{b_i\}$*

$$W_N^L(\{b_i\}; \{q_i\}) = \sum_{\{p_i\}} \hat{N}_{k,b}(\{b_i\}, \{p_i\}) N^{b-k+n} \prod_{i \geq 1} q_i^{p_i}. \quad (2.23)$$

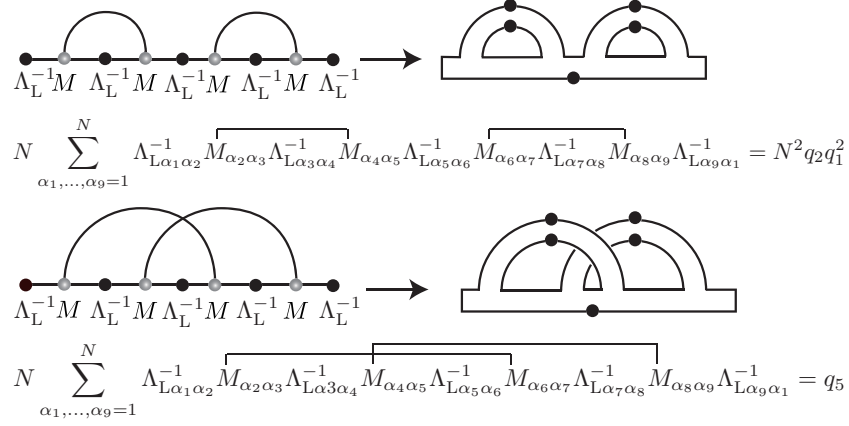


FIGURE 12. Chord diagrams of types $\{g, k; \{b_i\}; \{p_i\}\} = \{0, 2; b_5 = 1; p_1 = 2, p_3 = 1\}$ and $\{g, k; \{b_i\}; \{p_i\}\} = \{1, 2; b_5 = 1; p_5 = 1\}$.

We also consider the full generating function for the numbers $\hat{N}_{k,b}(\{b_i\}, \{p_i\})$ of chord diagrams

$$Z_N^L(y; \{s_i\}; \{q_i\}) = \sum_{\{b_i\}} \sum_{\{p_i\}} \hat{N}_{k,b}(\{b_i\}, \{p_i\}) N^{b-k+n} y^k \prod_{i \geq 0} s_i^{b_i} \prod_{i \geq 1} q_i^{p_i}.$$

This full generating function is given by the sum of Gaussian averages (2.21), and in consequence by the following Hermitian matrix integral

$$\begin{aligned} Z_N^L(y; \{s_i\}; \{q_i\}) &= \sum_{\{b_i\}} \frac{1}{\prod_i b_i!} y^k W_N^L(\{b_i\}, \{y^{-ib_i/2} q_i\}) \prod_i s_i^{b_i} \\ &= \frac{1}{\text{Vol}_N} \int_{\mathcal{H}_N} dM \exp \left[-N \text{Tr} \left(\frac{M^2}{2} - \sum_{i \geq 0} s_i y^{i/2} (\Lambda_L^{-1} M)^i \Lambda_L^{-1} \right) \right]. \end{aligned} \quad (2.24)$$

Comparing this matrix integral and the generating function $Z_N^L(y; \{s_i\}; \{q_i\})$ in equation (2.20), we arrive at the main theorem of this subsection.

Theorem 2.9. *The matrix integral (2.24) agrees with the generating function (2.20)*

$$Z_N^L(y; \{s_i\}; \{q_i\}) = Z^L(N^{-1}, y; \{s_i\}; \{q_i\}). \quad (2.25)$$

Specialization of the model. The cut-and-join equation for the numbers of chord diagrams is discussed in Subsection 3.2. For technical reasons, the partial differential equation for the generating function (2.20) with general parameter $\{s_i\}$ cannot be written in a simple form. Therefore we consider the specialization of the generating function (2.20) defined by⁴

$$s_i = s.$$

⁴ In [2], the length spectrum generating function $G_b(x, y; \{s_i\})$ is the same as in this specialized model.

Under this specialization, the matrix integral (2.24) reduces to

$$\begin{aligned} Z_N^L(y; s; \{q_i\}) &= Z_N^L(y; \{s_i = s\}; \{q_i\}) \\ &= \frac{1}{\text{Vol}_N} \int_{\mathcal{H}_N} dM \exp \left[-N \text{Tr} \left(\frac{M^2}{2} - \frac{s}{1 - y^{1/2} \Lambda_L^{-1} M} \Lambda_L^{-1} \right) \right]. \end{aligned} \quad (2.26)$$

For $Z^L(x, y; s; \{q_i\}) = Z^L(x, y; \{s_i = s\}; \{q_i\})$, we find

$$Z_N^L(y; s; \{q_i\}) = Z^L(N^{-1}, y; s; \{q_i\}). \quad (2.27)$$

In Subsection 3.2 we derive the cut-and-join equation for this specialized model, and show the agreement with the cut-and-join equation found by combinatorial means in [2].

2.3. The boundary length and point spectrum and the unified model. So far we have discussed separately the enumeration of chord diagrams and partial chord diagrams labeled by the boundary point spectrum and the boundary length spectrum. In this subsection we consider a unification of these two kinds of spectra, which is referred to as the boundary length and point spectrum. This unified spectrum was introduced and analyzed by cut-and-join methods in [7]. In what follows we construct a matrix model that encodes this new spectrum, and in Subsection 3.3 we show how the cut-and-join equation found in [7] follows from this matrix model.

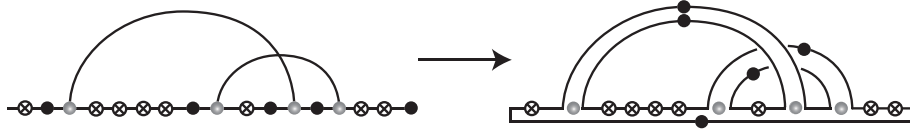


FIGURE 13. Decorating a partial chord diagram with the boundary label $\mathbf{i} = (1, 0, 1, 4, 2)$ with marked points for partitions.

The boundary length and point spectrum $\{n_{\mathbf{i}}\}$ is defined as follows [7].

Definition 2.10. Let c be a partial chord diagram. We associate the K tuple of numbers $\mathbf{i} = (i_1, i_2, \dots, i_K)$ to a boundary component of Σ_c , if we find the tuple \mathbf{i} of marked points around this boundary component, once we record different numbers of marked points in between chord ends and backbone underpasses along the boundary in the cyclic order induced from the orientation of Σ_c . The boundary length and point spectrum $\{n_{\mathbf{i}}\}$ counts the number of boundary cycles indexed by \mathbf{i} for the partial chord diagram c .

To enumerate the number of partial chord diagrams labeled by $\{g, k, l; \{b_i\}; \{n_{\mathbf{i}}\}\}$, we consider the generating functions introduced in [7].

Definition 2.11. Let $\mathcal{N}_{g,k,l}(\{b_i\}, \{n_{\mathbf{i}}\})$ denote the number of connected chord diagrams labeled by the set of parameters $(g, k, l; \{b_i\}; \{n_{\mathbf{i}}\})$ in the boundary length

and point spectrum. The generating function for these numbers is defined as

$$\begin{aligned}\mathcal{F}(x, y; \{s_i\}; \{u_{\mathbf{i}}\}) &= \sum_{b \geq 1} \mathcal{F}_b(x, y; \{s_i\}; \{u_{\mathbf{i}}\}), \\ \mathcal{F}_b(x, y; \{s_i\}; \{u_{\mathbf{i}}\}) &= \frac{1}{b!} \sum_{\sum_i b_i = b} \sum_{\{n_{\mathbf{i}}\}} \mathcal{N}_{g, k, l}(\{b_i\}, \{n_{\mathbf{i}}\}) x^{2g-2} y^k \prod_{i \geq 0} s_i^{b_i} \prod_{K \geq 1} \prod_{\{i_L\}_{L=1}^K} u_{\mathbf{i}}^{n_{\mathbf{i}}}.\end{aligned}\tag{2.28}$$

Exponentiating this generating function, one obtains the full generating function for the numbers $\hat{\mathcal{N}}_{k, b, l}(\{b_i\}, \{n_{\mathbf{i}}\})$ of partial chord diagrams

$$\begin{aligned}\mathcal{Z}(x, y; \{s_i\}; \{u_{\mathbf{i}}\}) &= \exp[\mathcal{F}(x, y; \{s_i\}; \{u_{\mathbf{i}}\})] \\ &= \sum_{\{b_i\}} \sum_{\{n_{\mathbf{i}}\}} \hat{\mathcal{N}}_{k, b, l}(\{b_i\}, \{n_{\mathbf{i}}\}) x^{-b+k-n} y^k \prod_{i \geq 0} s_i^{b_i} \prod_{K \geq 1} \prod_{\{i_L\}_{L=1}^K} u_{\mathbf{i}}^{n_{\mathbf{i}}},\end{aligned}\tag{2.29}$$

where l , k , and b obey

$$l = \sum_{K \geq 1} \sum_{\{i_L\}_{L=1}^K} \sum_{L=1}^K i_L n_{(i_1, \dots, i_K)}, \quad 2k + l = \sum_{i \geq 1} i b_i, \quad b = \sum_{i \geq 0} b_i.$$

The enumeration of partial chord diagrams decorated by the boundary length and point spectrum can also be expressed in terms of Gaussian averages over Hermitian matrices. To this end we again make use of extra marked points, just as in the previous section (concerning the length spectrum to mark the separation between marked points on the backbone, counted by the index \mathbf{i}), see Figure 13. Indeed, the boundary length and point spectrum also encodes the length spectrum, simply as the number K of partitions of marked points on boundary cycles.

To represent the boundary length and point spectrum, we introduce two external matrices Λ_P and Λ_L . In order to faithfully represent the ordering between marked points and partitions on each boundary cycle, we assume that these two external matrices do not commute

$$[\Lambda_P, \Lambda_L] \neq 0.$$

The correspondence between partial chord diagrams with the backbone spectrum $\{b_i\}$ and matchings by Wick contractions in a Gaussian average is given by a combination of the previous rules **C1**, **C2**, **P2**, **L2**, **P4**, **L4**, and **L5**. We summarize this correspondence in Table 1.

TABLE 1. The correspondence between partial chord diagrams with the backbone spectrum $\{b_i\}$ and matchings by Wick contractions in the Gaussian average.

A partial chord diagram	Gaussian average
A chord end on a backbone	$\Lambda_L^{-1} M$
A marked point on a backbone	Λ_P
An underside of a backbone	$N \Lambda_L^{-1}$
A backbone	$N \text{Tr} (\Lambda_L^{-1} \Lambda_P^{\alpha_1} \Lambda_L^{-1} \Lambda_P^{\alpha_2} \Lambda_L^{-1} \cdots \Lambda_P^{\alpha_K} \Lambda_L^{-1})$
A chord	Wick contraction \overbrace{MM}

Based on these rules, one finds a bijective correspondence between partial chord diagrams with the backbone spectrum $\{b_i\}$ and matchings by Wick contractions in the Gaussian average

$$\mathcal{W}_N(\{b_i\}; \{u_i\}) = \left\langle \prod_{i \geq 0} (N \text{Tr}(\Lambda_L^{-1} M + \Lambda_P)^i \Lambda_L^{-1})^{b_i} \right\rangle_N^G, \quad (2.30)$$

where in order to represent trace factors Λ_P and Λ_L we introduced the *generalized Miwa times*

$$u_{(i_1, \dots, i_K)} = \frac{1}{N} \text{Tr}(\Lambda_P^{i_1} \Lambda_L^{-1} \Lambda_P^{i_2} \Lambda_L^{-1} \dots \Lambda_P^{i_K} \Lambda_L^{-1}). \quad (2.31)$$

If a partial chord diagram c contains a boundary cycle labeled by $\mathbf{i} = (i_1, \dots, i_K)$, one finds the following trace factor in the corresponding Wick contractions in $\mathcal{W}_N(\{b_i\}; \{u_i\})$

$$\text{Tr}(\Lambda_P^{i_1} \Lambda_L^{-1} \Lambda_P^{i_2} \Lambda_L^{-1} \dots \Lambda_P^{i_K} \Lambda_L^{-1}).$$

Finally, combining Propositions 2.5 and 2.8, we obtain the key proposition.

Proposition 2.12. *The Gaussian average $\mathcal{W}_N(\{b_i\}; \{u_i\})$ in the equation (2.30) is the generating function for the numbers $\widehat{\mathcal{N}}_{k,b,l}(\{b_i\}, \{n_i\})$ of partial chord diagrams*

$$\mathcal{W}_N(\{b_i\}; \{u_i\}) = \sum_{\{n_i\}} \widehat{\mathcal{N}}_{k,b,l}(\{b_i\}, \{n_i\}) N^{b-k+n} \prod_{K \geq 1} \prod_{\{i_L\}_{L=1}^K} u_i^{n_i}. \quad (2.32)$$

Repeating the same combinatorics as in the previous subsections, we find the main theorem of this section.

Theorem 2.13. *The Hermitian matrix integral*

$$\begin{aligned} \mathcal{Z}_N(y; \{s_i\}; \{u_i\}) &= \\ &= \frac{1}{\text{Vol}_N} \int dM \exp \left[-N \text{Tr} \left(\frac{M^2}{2} - \sum_{i \geq 0} s_i (y^{1/2} \Lambda_L^{-1} M + \Lambda_P)^i \Lambda_L^{-1} \right) \right] \end{aligned} \quad (2.33)$$

agrees with the generating function (2.29)

$$\mathcal{Z}_N(y; \{s_i\}; \{u_i\}) = \mathcal{Z}(N^{-1}, y; \{s_i\}; \{u_i\}). \quad (2.34)$$

3. CUT-AND-JOIN EQUATIONS VIA MATRIX MODELS

In Section 2 we discussed matrix models that enumerate partial chord diagrams filtered by the boundary point spectrum, the boundary length spectrum, and the boundary length and point spectrum. In this section we derive partial differential equations for these matrix models, and show that they agree with the cut-and-join equations found in [2, 7]. To derive these differential equations, it is useful to introduce the following matrix integral.

Definition 3.1. Let A and B denote invertible matrices of rank N . We define a formal matrix integral with parameters y , $\{g_i\}_{i=-\infty}^{+\infty}$, and matrices A and B , as follows

$$\begin{aligned} Z_N(y; \{g_i\}; A; B) &= \\ &= \frac{1}{\text{Vol}_N} \int_{\mathcal{H}_N} dM \exp \left[-N \text{Tr} \left(\frac{1}{2} M^2 - \sum_{i \in \mathbb{Z}} g_i (y^{1/2} B^{-1} M + A)^i B^{-1} \right) \right]. \end{aligned} \quad (3.1)$$

By the following specializations of this matrix integral one finds matrix integrals discussed in Section 2

$$\begin{aligned} Z_N^P(y; \{s_i\}; \{r_i\}) : \quad & g_{i<0} = 0, \quad g_{i\geq 0} = s_i, \quad A = \Lambda_P, \quad B = I_N, \\ Z_N^L(y; \{s_i\}; \{q_i\}) : \quad & g_{i<0} = 0, \quad g_{i\geq 0} = s_i, \quad A = 0, \quad B = \Lambda_L, \\ Z_N^L(y; s; \{q_i\}) : \quad & g_{i\neq -1} = 0, \quad g_{-1} = -s, \quad A = \Lambda_L, \quad B = -I_N, \\ Z_N(y; \{s_i\}; \{u_i\}) : \quad & g_{i<0} = 0, \quad g_{i\geq 0} = s_i, \quad A = \Lambda_P, \quad B = \Lambda_L, \end{aligned}$$

where I_N is the rank N identity matrix.

The matrix integral (3.1) satisfies the following partial differential equation.

Proposition 3.2. *The matrix integral $Z_N(y; \{g_i\}; A; B)$ obeys a partial differential equation*

$$\left[\frac{\partial}{\partial y} - \frac{1}{2N} \text{Tr}(B^{-1})^T \frac{\partial}{\partial A} (B^{-1})^T \frac{\partial}{\partial A} \right] Z_N(y; \{g_i\}; A; B) = 0, \quad (3.2)$$

where the trace in the second term is defined, for rank N matrices X and Y , as

$$\text{Tr} X \frac{\partial}{\partial Y} = \sum_{\alpha, \beta=1}^N X_{\alpha\beta} \frac{\partial}{\partial Y_{\beta\alpha}}.$$

Proof. By a shift $M = X - y^{-1/2}BA$, the matrix integral (3.1) can be rewritten as

$$\begin{aligned} Z_N(y; \{g_i\}; A; B) &= \\ &= \frac{1}{\text{Vol}_N} \int_{\tilde{\mathcal{H}}_N} dX \exp \left[-N \text{Tr} \left(\frac{1}{2} (X - y^{-1/2}BA)^2 - \sum_{i \in \mathbb{Z}} y^{i/2} g_i (B^{-1}X)^i B^{-1} \right) \right]. \end{aligned} \quad (3.3)$$

Here $\tilde{\mathcal{H}}_N$ is the space of shifted matrices $X = M + y^{-1/2}BA$ with $M \in \mathcal{H}_N$. The invariance of this matrix integral under the infinitesimal scaling $X_{\alpha\beta} \rightarrow (1 + \epsilon)X_{\alpha\beta}$ leads to a constraint equation

$$\left\langle N^2 - N \text{Tr} X^2 + y^{-1/2} N \text{Tr} BAX + N \sum_{i \in \mathbb{Z}} i y^{i/2} g_i \text{Tr}(B^{-1}X)^i B^{-1} \right\rangle = 0, \quad (3.4)$$

where the first term N^2 comes from the measure factor, as $dX \rightarrow (1 + N^2\epsilon)dX$. Here we have defined the unnormalized average for an observable $\mathcal{O}(X)$

$$\langle \mathcal{O}(X) \rangle = \int_{\tilde{\mathcal{H}}_N} dX \mathcal{O}(X) \exp \left[-N \text{Tr} \left(\frac{1}{2} (X - y^{-1/2}BA)^2 - \sum_{i \in \mathbb{Z}} y^{i/2} g_i (B^{-1}X)^i B^{-1} \right) \right].$$

Using

$$\begin{aligned} \frac{1}{N} y^{1/2} \sum_{\gamma=1}^N (B^{-1})_{\beta\gamma}^T \frac{\partial}{\partial A_{\gamma\alpha}} Z_N(y; \{g_i\}; A; B) &= \left\langle X_{\alpha\beta} - y^{-1/2} N \sum_{\gamma=1}^N B_{\alpha\gamma} A_{\gamma\beta} \right\rangle, \\ \frac{1}{N} \frac{\partial}{\partial g_i} Z_N(y; \{g_i\}; A; B) &= y^{i/2} \langle \text{Tr}(B^{-1}X)^i B^{-1} \rangle, \end{aligned}$$

one finds that the constraint equation (3.4) yields

$$\left[-\frac{1}{N} y \text{Tr}(B^{-1})^T \frac{\partial}{\partial A} (B^{-1})^T \frac{\partial}{\partial A} - \text{Tr} A^T \frac{\partial}{\partial A} + \sum_{i \in \mathbb{Z}} i g_i \frac{\partial}{\partial g_i} \right] Z_N(y; \{g_i\}; A; B) = 0.$$

It follows from (3.3) that the last two derivatives in the expression above can be replaced by $2y\partial/\partial y$, so that the partial differential equation (3.2) is obtained. \square

Remark 3.3. In the above proof of the constraint equation (3.4) we considered the infinitesimal scaling $X_{\alpha\beta} \rightarrow (1 + \epsilon)X_{\alpha\beta}$. More generally, matrix integral (3.3) is invariant under infinitesimal shifts

$$X_{\alpha\beta} \longrightarrow X_{\alpha\beta} + \epsilon(X^{n+1})_{\alpha\beta}, \quad n = -1, 0, 1, \dots$$

It is known that for the matrix integral without external matrices A and B this symmetry yields the Virasoro symmetry, and in particular the scaling $X_{\alpha\beta} \rightarrow (1 + \epsilon)X_{\alpha\beta}$ is related to the Virasoro generator L_0^{Vir} [22, 19].⁵

3.1. The boundary point spectrum. In Subsection 2.1 we showed that the matrix integral $Z_N^{\text{P}}(y; \{s_i\}; \{r_i\})$ in (2.17)

$$\begin{aligned} Z_N^{\text{P}}(y; \{s_i\}; \{r_i\}) &= \\ &= \frac{1}{\text{Vol}_N} \int_{\mathcal{H}_N} dM \exp \left[-N \text{Tr} \left(\frac{M^2}{2} - \sum_{i \geq 0} s_i y^{i/2} (M + y^{-1/2} \Lambda_{\text{P}})^i \right) \right], \end{aligned}$$

enumerates partial chord diagrams labeled by the boundary point spectrum. By the specialization

$$g_{i < 0} = 0, \quad g_{i \geq 0} = s_i, \quad A = \Lambda_{\text{P}}, \quad B = I_N = \text{identity matrix},$$

of the matrix integral $Z_N(y; \{g_i\}; A; B)$ in (3.1) we see that

$$Z_N(y; s_{i < 0} = 0, \{s_i\}_{i \geq 0}; \Lambda_{\text{P}}; I_N) = Z_N^{\text{P}}(y; \{s_i\}; \{r_i\}), \quad (3.5)$$

where the reverse Miwa times r_i are defined in (2.15). From (3.2) we obtain the partial differential equation satisfied by $Z_N^{\text{P}}(y; \{s_i\}; \{r_i\})$.

Corollary 3.4. *The matrix integral $Z_N^{\text{P}}(y; \{s_i\}; \{r_i\})$ obeys the partial differential equation*

$$\left[\frac{\partial}{\partial y} - \frac{1}{2N} \text{Tr} \frac{\partial^2}{\partial \Lambda_{\text{P}}^2} \right] Z_N^{\text{P}}(y; \{s_i\}; \{r_i\}) = 0. \quad (3.6)$$

This corollary implies the following theorem.

Theorem 3.5. *Let L_0 and L_2 be the differential operators⁶*

$$\begin{aligned} L_0 &= \frac{1}{2} \sum_{i \geq 2} \sum_{j=0}^{i-2} i r_j r_{i-j-2} \frac{\partial}{\partial r_i}, \\ L_2 &= \frac{1}{2} \sum_{i \geq 2} \sum_{j=1}^{i-1} j(i-j) r_{i-2} \frac{\partial^2}{\partial r_i \partial r_{i-j}}. \end{aligned} \quad (3.7)$$

The matrix integral $Z_N^{\text{P}}(y; \{s_i\}; \{r_i\})$ obeys the cut-and-join equation

$$\frac{\partial}{\partial y} Z_N^{\text{P}}(y; \{s_i\}; \{r_i\}) = \mathcal{L} Z_N^{\text{P}}(y; \{s_i\}; \{r_i\}), \quad (3.8)$$

⁵ In [33, 18], the Schwinger-Dyson approach to the enumeration of chord diagrams is also discussed.

⁶ In [36] the differential operators L_0 and L_2 were denoted by $W^{(3)}$.

where

$$\mathcal{L} = L_0 + \frac{1}{N^2} L_2.$$

The formal solution of this cut-and-join equation, which gives the matrix integral $Z_N^P(y; \{s_i\}; \{r_i\})$, is iteratively determined from the initial condition at $y = 0$,

$$Z_N^P(y; \{s_i\}; \{r_i\}) = e^{y\mathcal{L}} Z_N^P(0; \{s_i\}; \{r_i\}) = e^{y\mathcal{L}} e^{N^2 \sum_{i \geq 0} s_i r_i}. \quad (3.9)$$

This theorem follows from the lemma below by rewriting the derivative $\text{Tr} \partial^2 / \partial \Lambda_P^2$ in the partial differential equation (3.6).

Lemma 3.6. *For a function $f(\{r_i\})$ of the reverse Miwa times r_i , the derivative $\text{Tr} \partial^2 / \partial \Lambda_P^2$ can be rewritten as*

$$\frac{1}{2N} \text{Tr} \frac{\partial^2}{\partial \Lambda_P^2} f(\{r_i\}) = \left(L_0 + \frac{1}{N^2} L_2 \right) f(\{r_i\}). \quad (3.10)$$

Proof. Consider the derivative $\partial / \partial \Lambda_{P\beta\alpha}$ of r_i ,

$$\frac{\partial r_i}{\partial \Lambda_{P\beta\alpha}} = \frac{i}{N} \Lambda_{P\alpha\beta}^{i-1}, \quad \text{Tr} \frac{\partial^2 r_i}{\partial \Lambda_P^2} = iN \sum_{j=0}^{i-2} r_j r_{i-j-2}.$$

Then the derivative $\text{Tr} \partial^2 / \partial \Lambda_P^2$ of the function $f(\{r_i\})$ is re-expressed as

$$\begin{aligned} \frac{1}{2N} \text{Tr} \frac{\partial^2}{\partial \Lambda_P^2} f(\{r_i\}) &= \frac{1}{2N} \sum_{i \geq 0} \text{Tr} \frac{\partial^2 r_i}{\partial \Lambda_P^2} \frac{\partial f(\{r_i\})}{\partial r_i} + \frac{1}{2N} \sum_{i,j \geq 0} \sum_{\alpha, \beta=1}^N \frac{\partial r_i}{\partial \Lambda_{P\beta\alpha}} \frac{\partial r_j}{\partial \Lambda_{P\alpha\beta}} \frac{\partial^2 f(\{r_i\})}{\partial r_i \partial r_j} \\ &= \frac{1}{2} \sum_{i \geq 2} \sum_{j=0}^{i-2} i r_j r_{i-j-2} \frac{\partial f(\{r_i\})}{\partial r_i} + \frac{1}{2N^2} \sum_{i,j \geq 1} i j r_{i+j-2} \frac{\partial^2 f(\{r_i\})}{\partial r_i \partial r_j}. \end{aligned}$$

This coincides with the right hand side of (3.10). \square

The cut-and-join equation for the rescaled matrix integral (2.18) yields

$$\frac{\partial}{\partial y} Z_{t_0 N}^P(t_0 y; \{t_0^{-1} s_i\}; \{t_0^{-1} t_i\}) = \mathcal{L} Z_{t_0 N}^P(t_0 y; \{t_0^{-1} s_i\}; \{t_0^{-1} t_i\}), \quad (3.11)$$

where \mathcal{L} is given by

$$\begin{aligned} \mathcal{L} &= L_0 + x^2 L_2, \quad x = N^{-1}, \\ L_0 &= \frac{1}{2} \sum_{i \geq 2} \sum_{j=0}^{i-2} i t_j t_{i-j-2} \frac{\partial}{\partial t_i}, \quad L_2 = \frac{1}{2} \sum_{i \geq 2} \sum_{j=1}^{i-1} j(i-j) t_{i-2} \frac{\partial^2}{\partial t_i \partial t_{i-j}}. \end{aligned} \quad (3.12)$$

This cut-and-join equation agrees with the partial differential equation in Theorem 1 of [2], where it was proven combinatorially by the recursion relation for the number of partial chord diagrams.⁷ This completes the proof of Theorem 2.6.

⁷For the Grothendieck's dessin counting, a similar cut-and-join equation was found in [27].

3.2. The boundary length spectrum. In Subsection 2.2 we showed that the matrix integral $Z_N^L(y; \{s_i\}; \{q_i\})$ in (2.24) enumerates chord diagrams labeled by the boundary length spectrum. By the specialization

$$g_{i<0} = 0, \quad g_{i\geq 0} = s_i, \quad A = 0, \quad B = \Lambda_L,$$

of the matrix integral $Z_N(y; \{g_i\}; A; B)$ in (3.1) we see that

$$Z_N(y; s_{i<0} = 0, \{s_i\}_{i\geq 0}; \Lambda_L) = Z_N^L(y; \{s_i\}; \{q_i\}), \quad (3.13)$$

where the Miwa times q_i are defined in equation (2.22).

Obviously, for $A = 0$ the partial differential equation (3.2) does not hold. Instead we consider the matrix integral (2.26) obtained by the specialization $s_i = s$

$$Z_N^L(y; s; \{q_i\}) = \frac{1}{\text{Vol}_N} \int_{\mathcal{H}_N} dM \exp \left[-N \text{Tr} \left(\frac{M^2}{2} + \frac{s}{y^{1/2}M - \Lambda_L} \right) \right].$$

The same matrix integral can be obtained by the specialization

$$g_{i\neq -1} = 0, \quad g_{-1} = -s, \quad A = \Lambda_L, \quad B = -I_N,$$

and thus

$$Z_N(y; s_i = -\delta_{i,-1}; \Lambda_L; B = -I_N) = Z_N^L(y; s; \{q_i\}). \quad (3.14)$$

Then from (3.2) we obtain a partial differential equation for $Z_N^L(y; s; \{q_i\})$.

Corollary 3.7. *The matrix integral $Z_N^L(y; s; \{q_i\})$ obeys the partial differential equation*

$$\left[\frac{\partial}{\partial y} - \frac{1}{2N} \text{Tr} \frac{\partial^2}{\partial \Lambda_L^2} \right] Z_N^L(y; s; \{r_i\}) = 0. \quad (3.15)$$

This corollary implies the following theorem.

Theorem 3.8. *Let K_0 and K_2 be the differential operators*

$$\begin{aligned} K_0 &= \frac{1}{2} \sum_{i\geq 3} \sum_{j=1}^{i-1} (i-2) q_j q_{i-j} \frac{\partial}{\partial q_{i-2}}, \\ K_2 &= \frac{1}{2} \sum_{i\geq 2} \sum_{j=1}^{i-1} j(i-j) q_{i+2} \frac{\partial^2}{\partial q_i \partial q_{i-j}}. \end{aligned} \quad (3.16)$$

The matrix integral $Z_N^L(y; s; \{q_i\})$ obeys the cut-and-join equation

$$\frac{\partial}{\partial y} Z_N^L(y; s; \{q_i\}) = \mathcal{K} Z_N^L(y; s; \{q_i\}), \quad (3.17)$$

where

$$\mathcal{K} = K_0 + \frac{1}{N^2} K_2.$$

The formal solution of this cut-and-join equation, which gives the matrix integral $Z_N^L(y; s; \{q_i\})$, is iteratively determined from the initial condition at $y = 0$,

$$Z_N^L(y; s; \{q_i\}) = e^{y\mathcal{K}} Z_N^L(y = 0; s; \{q_i\}) = e^{y\mathcal{K}} e^{N^2 s q_1}. \quad (3.18)$$

The cut-and-join equation (3.17) was combinatorially proven in Theorem 2 of [2] for the generating function $Z^L(x, y; s; \{q_i\})$ in (2.19), and thus Theorem 2.9 for $s_i = s$ is reproved.

The claim of Theorem 3.8 is proven by rewriting the derivative $\text{Tr} \partial^2 / \partial \Lambda_L^2$ in the partial differential equation (3.15) using the following lemma.

Lemma 3.9. *For a function $g(\{q_i\})$ of the Miwa times $\{q_i\}$, the derivative $\text{Tr} \partial^2 / \partial \Lambda_L^2$ can be rewritten as follows*

$$\frac{1}{2N} \text{Tr} \frac{\partial^2}{\partial \Lambda_L^2} g(\{q_i\}) = \left(K_0 + \frac{1}{N^2} K_2 \right) g(\{q_i\}). \quad (3.19)$$

Proof. By acting $\partial / \partial \Lambda_L$ on the Miwa time q_i one obtains

$$\frac{\partial q_i}{\partial \Lambda_{L\alpha\beta}} = -\frac{i}{N} \Lambda_{L\beta\alpha}^{-i-1}, \quad \text{Tr} \frac{\partial^2 q_i}{\partial \Lambda_L^2} = iN \sum_{j=1}^{i+1} q_j q_{i-j+2}.$$

Adopting this relation via the chain rule applied to the Λ_L derivatives, one finds that

$$\begin{aligned} \frac{1}{2N} \text{Tr} \frac{\partial^2 g(\{q_i\})}{\partial \Lambda_L^2} &= \frac{1}{2N} \sum_{i \geq 0} \text{Tr} \frac{\partial^2 q_i}{\partial \Lambda_L^2} \frac{\partial g(\{q_i\})}{\partial q_i} + \frac{1}{2N} \sum_{i,j \geq 0} \sum_{\alpha, \beta=1}^N \frac{\partial q_i}{\partial \Lambda_{L\alpha\beta}} \frac{\partial q_j}{\partial \Lambda_{L\beta\alpha}} \frac{\partial^2 g(\{q_i\})}{\partial q_i \partial q_j} \\ &= \frac{1}{2} \sum_{i \geq 1} i q_j q_{i-j+2} \frac{\partial g(\{q_i\})}{\partial q_i} + \frac{1}{2N^2} \sum_{i,j \geq 1} i j q_{i+j+2} \frac{\partial^2 g(\{q_i\})}{\partial q_i \partial q_j}. \end{aligned}$$

This coincides with the right hand side of (3.19). \square

3.3. The boundary length and point spectrum. In Subsection 2.3 we showed that the matrix integral $\mathcal{Z}_N(y; \{s_i\}; \{u_i\})$ in (2.29)

$$\begin{aligned} \mathcal{Z}_N(y; \{s_i\}; \{u_i\}) &= \\ &= \frac{1}{\text{Vol}_N} \int_{\mathcal{H}_N} dM \exp \left[-N \text{Tr} \left(\frac{M^2}{2} - \sum_{i \geq 0} s_i (y^{1/2} \Lambda_L^{-1} M + \Lambda_P)^i \Lambda_L^{-1} \right) \right] \end{aligned}$$

enumerates partial chord diagrams labeled by the boundary length and point spectrum. By the specialization

$$g_{i < 0} = 0, \quad g_{i \geq 0} = s_i, \quad A = \Lambda_P, \quad B = \Lambda_L,$$

of the matrix integral $Z_N(y; \{g_i\}; A; B)$ in (3.1) we see that

$$Z_N(y; s_{i < 0} = 0, \{s_i\}_{i \geq 0}; \Lambda_P; \Lambda_L) = \mathcal{Z}_N(y; \{s_i\}; \{u_i\}), \quad (3.20)$$

where the generalized Miwa times $u_{(i_1, \dots, i_K)}$ are defined in (2.31)

$$u_{(i_1, \dots, i_K)} = \frac{1}{N} \text{Tr} (\Lambda_P^{i_1} \Lambda_L^{-1} \Lambda_P^{i_2} \Lambda_L^{-1} \cdots \Lambda_P^{i_K} \Lambda_L^{-1}).$$

From (3.2) we obtain a partial differential equation for $\mathcal{Z}_N(y; \{s_i\}; \{u_i\})$.

Corollary 3.10. *The matrix integral $\mathcal{Z}_N(y; \{s_i\}; \{u_i\})$ obeys the partial differential equation*

$$\left[\frac{\partial}{\partial y} - \frac{1}{2N} \text{Tr} (\Lambda_L^{-1})^T \frac{\partial}{\partial \Lambda_P} (\Lambda_L^{-1})^T \frac{\partial}{\partial \Lambda_P} \right] \mathcal{Z}_N(y; \{s_i\}; \{u_i\}) = 0. \quad (3.21)$$

This corollary implies the following main theorem of this section.

Theorem 3.11. *Let M_0 and M_2 be the following differential operators with respect to parameters $u_{\mathbf{i}}$*

$$\begin{aligned}
M_0 &= \frac{1}{2} \sum_{K \geq 1} \sum_{\{i_1, \dots, i_K\}} \sum_{1 \leq I \neq M \leq K} \sum_{\ell=0}^{i_I-1} \sum_{m=0}^{i_M-1} \\
&\quad u_{(i_I-\ell-1, i_{I+1}, \dots, i_{M-1}, m)} u_{(i_M-m-1, i_{M+1}, \dots, i_{I-1}, \ell)} \frac{\partial}{\partial u_{(i_1, \dots, i_K)}} \\
&\quad + \sum_{K \geq 1} \sum_{\{i_1, \dots, i_K\}} \sum_{I=0}^K \sum_{\ell+m \leq i_I-2} u_{(\ell, m, i_{I+1}, \dots, i_{I-1})} u_{(i_I-\ell-m-2)} \frac{\partial}{\partial u_{(i_1, \dots, i_K)}}, \\
M_2 &= \frac{1}{2} \sum_{K, L \geq 0} \sum_{\{i_1, \dots, i_K\}} \sum_{\{j_1, \dots, j_L\}} \sum_{I=0}^K \sum_{J=0}^L \sum_{\ell=0}^{i_I-1} \sum_{m=0}^{j_J-1} \\
&\quad u_{(i_I-\ell-1, i_{I+1}, \dots, i_{I-1}, \ell, j_J-m-1, j_{J+1}, \dots, j_{J-1}, m)} \frac{\partial^2}{\partial u_{(i_1, \dots, i_K)} \partial u_{(j_1, \dots, j_L)}}, \tag{3.22}
\end{aligned}$$

where labels I, M 's are defined modulo K , and the label J is defined modulo L . The matrix integral $\mathcal{Z}_N(y; \{s_i\}; \{u_{\mathbf{i}}\})$ obeys the cut-and-join equation

$$\frac{\partial}{\partial y} \mathcal{Z}_N(y; \{s_i\}; \{u_{\mathbf{i}}\}) = \mathcal{M} \mathcal{Z}_N(y; \{s_i\}; \{u_{\mathbf{i}}\}), \tag{3.23}$$

where

$$\mathcal{M} = M_0 + \frac{1}{N^2} M_2.$$

The formal solution of this cut-and-join equation, which gives the matrix integral $\mathcal{Z}_N(y; \{s_i\}; \{u_{\mathbf{i}}\})$, is iteratively determined from the initial condition at $y = 0$,

$$\mathcal{Z}_N(y; \{s_i\}; \{u_{\mathbf{i}}\}) = e^{y\mathcal{M}} \mathcal{Z}_N(y=0; \{s_i\}; \{u_{\mathbf{i}}\}) = e^{y\mathcal{M}} e^{N^2 \sum_{i \geq 0} s_i u_{(i)}}. \tag{3.24}$$

The partial differential equation (3.23) agrees with the cut-and-join equation obtained combinatorially in Theorem 1.1 of [7]. Here we prove this theorem by rewriting the derivative in the second term of the partial differential equation (3.21), taking advantage of the following lemma.

Lemma 3.12. *For a function $h(\{u_{\mathbf{i}}\})$ of the generalized Miwa times $u_{\mathbf{i}}$, the derivative in the second term of the partial differential equation (3.21) can be rewritten as follows*

$$\frac{1}{2N} \text{Tr} \left[(\Lambda_L^{-1})^T \frac{\partial}{\partial \Lambda_P} (\Lambda_L^{-1})^T \frac{\partial}{\partial \Lambda_P} \right] h(\{u_{\mathbf{i}}\}) = \left(M_0 + \frac{1}{N^2} M_2 \right) h(\{u_{\mathbf{i}}\}). \tag{3.25}$$

Proof. By the chain rule, the derivative on the left hand side of (3.25) is rewritten as follows

$$\begin{aligned}
& \text{Tr} \left[(\Lambda_L^{-1})^T \frac{\partial}{\partial \Lambda_P} (\Lambda_L^{-1})^T \frac{\partial}{\partial \Lambda_P} \right] h(\{u_i\}) = \\
& = \sum_{K \geq 0} \sum_{(i_1, \dots, i_K)} \text{Tr} \left[(\Lambda_L^{-1})^T \frac{\partial}{\partial \Lambda_P} (\Lambda_L^{-1})^T \frac{\partial}{\partial \Lambda_P} u_{(i_1, \dots, i_K)} \right] \frac{\partial}{\partial u_{(i_1, \dots, i_K)}} h(\{u_i\}) \\
& + \sum_{K, L \geq 0} \sum_{(i_1, \dots, i_K)} \sum_{(j_1, \dots, j_L)} \text{Tr} \left[(\Lambda_L^{-1})^T \frac{\partial}{\partial \Lambda_P} u_{(i_1, \dots, i_K)} (\Lambda_L^{-1})^T \frac{\partial}{\partial \Lambda_P} u_{(j_1, \dots, j_L)} \right] \\
& \quad \times \frac{\partial^2}{\partial u_{(i_1, \dots, i_K)} \partial u_{(j_1, \dots, j_L)}} h(\{u_i\}).
\end{aligned}$$

Each of the coefficients yields

$$\begin{aligned}
& \text{Tr} \left[(\Lambda_L^{-1})^T \frac{\partial}{\partial \Lambda_P} (\Lambda_L^{-1})^T \frac{\partial}{\partial \Lambda_P} u_{(i_1, \dots, i_K)} \right] = \\
& = \sum_{1 \leq I \neq M \leq K} \sum_{\ell=0}^{i_I-1} \sum_{m=0}^{i_M-1} \frac{1}{N} \text{Tr}(\Lambda_P^{i_I-\ell-1} \Lambda_L^{-1} \Lambda_P^{i_{I+1}} \Lambda_L^{-1} \dots \Lambda_P^{i_M-1} \Lambda_L^{-1} \Lambda_P^m \Lambda_L^{-1}) \\
& \quad \times \text{Tr}(\Lambda_P^{i_M-m-1} \Lambda_L^{-1} \Lambda_P^{i_{M+1}} \Lambda_L^{-1} \dots \Lambda_P^{i_I-1} \Lambda_L^{-1} \Lambda_P^\ell \Lambda_L^{-1}) \\
& + 2 \sum_{L=0}^K \sum_{\ell+m \leq i_I-2} \frac{1}{N} \text{Tr}(\Lambda_P^\ell \Lambda_L^{-1} \Lambda_P^m \Lambda_L^{-1} \Lambda_P^{i_{I+1}} \Lambda_L^{-1} \dots \Lambda_P^{i_L-1} \Lambda_L^{-1}) \text{Tr}(\Lambda_P^{i_I-\ell-m-2} \Lambda_L^{-1}) \\
& = N \sum_{1 \leq I \neq M \leq K} \sum_{\ell=0}^{i_I-1} \sum_{m=0}^{i_M-1} u_{(i_I-\ell-1, i_{I+1}, \dots, i_{M-1}, m)} u_{(i_M-m-1, i_{M+1}, \dots, i_{I-1}, \ell)} \\
& + 2N \sum_{L=0}^K \sum_{\ell+m \leq i_I-2} u_{(\ell, m, i_{I+1}, \dots, i_{I-1})} u_{(i_I-\ell-m-2)},
\end{aligned}$$

and

$$\begin{aligned}
& \text{Tr} \left[(\Lambda_L^{-1})^T \frac{\partial}{\partial \Lambda_P} u_{(i_1, \dots, i_K)} (\Lambda_L^{-1})^T \frac{\partial}{\partial \Lambda_P} u_{(j_1, \dots, j_L)} \right] = \\
& = \sum_{I=1}^K \sum_{J=1}^L \sum_{\ell=0}^{i_I-1} \sum_{m=0}^{j_J-1} \frac{1}{N^2} \text{Tr}(\Lambda_P^{i_I-\ell-1} \Lambda_L^{-1} \Lambda_P^{i_{I+1}} \Lambda_L^{-1} \dots \Lambda_P^{i_I-1} \Lambda_L^{-1} \Lambda_P^\ell \Lambda_L^{-1} \\
& \quad \cdot \Lambda_P^{j_J-m-1} \Lambda_L^{-1} \Lambda_P^{j_{J+1}} \Lambda_L^{-1} \dots \Lambda_P^{j_J-1} \Lambda_L^{-1} \Lambda_P^m \Lambda_L^{-1}) \\
& = \frac{1}{N} \sum_{I=1}^K \sum_{J=1}^L \sum_{\ell=0}^{i_I-1} \sum_{m=0}^{j_J-1} u_{(i_I-\ell-1, i_{I+1}, \dots, i_{I-1}, \ell, j_J-m-1, j_{J+1}, \dots, j_{J-1}, m)}.
\end{aligned}$$

In this way one obtains the right hand side of (3.25). \square

As a corollary of Theorem 3.11, one finds the cut-and-join equation for the 1-backbone generating function.⁸

⁸For $\Lambda_L = I_N$ (or $s_i = s$ and $\Lambda_P = 0$) the cut-and-join equation for the 1-backbone generating function labeled by the boundary point spectrum (or boundary length spectrum) was proven combinatorially in [2].

Corollary 3.13. *The 1-backbone generating function $\mathcal{F}_1(x, y; \{s_i\}; \{u_i\})$ obtained by picking up the $\mathcal{O}(s_i^1)$ terms in $\mathcal{Z}_N(y; \{s_i\}; \{u_i\})$ as follows*

$$\begin{aligned} \mathcal{F}_1(N^{-1}, y; \{s_i\}; \{u_i\}) \\ = \frac{1}{\text{Vol}_N} \int_{\mathcal{H}_N} dM e^{-N \text{Tr} \frac{M^2}{2}} N \sum_{i \geq 0} s_i \text{Tr}(y^{1/2} \Lambda_L^{-1} M + \Lambda_P)^i \Lambda_L^{-1}, \end{aligned} \quad (3.26)$$

obeys the cut-and-join equation

$$\frac{\partial}{\partial y} \mathcal{F}_1(x, y; \{s_i\}; \{u_i\}) = \mathcal{M} \mathcal{F}_1(x, y; \{s_i\}; \{u_i\}), \quad (3.27)$$

where $\mathcal{M} = M_0 + x^2 M_2$. The solution is iteratively determined by

$$\mathcal{F}_1(x, y; \{s_i\}; \{u_i\}) = e^{y\mathcal{M}} \mathcal{F}_1(x, y=0; \{s_i\}; \{u_i\}) = e^{y\mathcal{M}} \left(x^{-2} \sum_{i \geq 0} s_i u_{(i)} \right). \quad (3.28)$$

4. NON-ORIENTED ANALOGUES

In this section we consider the enumeration of both orientable and non-orientable (jointly called non-oriented) partial chord diagrams [2, 7]. To this end we generalize the matrix models introduced in Section 2. In Subsection 4.1, matrix models for the boundary point spectrum, the boundary length spectrum, and the boundary length and point spectrum are introduced, based on the corresponding Gaussian matrix integrals over the space of rank N real symmetric matrices. Subsequently, in Subsection 4.2, we derive cut-and-join equations for the generating functions of non-oriented partial chord diagrams, using analogous methods as those discussed in Section 3.

4.1. Non-oriented analogues of the matrix models. In this subsection we generalize matrix models found in Section 2, in order to enumerate both orientable and non-orientable partial chord diagrams [2, 7].

Definition 4.1. Let $\tilde{\mathcal{N}}_{h,k,l}(\{b_i\}, \{n_i\}, \{p_i\})$ denote the number of connected non-oriented partial chord diagrams of type $\{h, k, l; \{b_i\}; \{n_i\}; \{p_i\}\}$. Analogously as in the orientable case, we define

$$\begin{aligned} \tilde{\mathcal{N}}_{h,k,l}(\{b_i\}, \{n_i\}) &= \sum_{\{p_i\}} \tilde{\mathcal{N}}_{h,k,l}(\{b_i\}, \{n_i\}, \{p_i\}), \\ \tilde{\mathcal{N}}_{h,k}(\{b_i\}, \{p_i\}) &= \sum_{\{n_i\}} \tilde{\mathcal{N}}_{h,k,l=0}(\{b_i\}, \{n_i\}, \{p_i\}), \end{aligned}$$

and introduce generating functions

$$\begin{aligned} \tilde{F}(x, y; \{s_i\}; \{t_i\}) &= \sum_{b \geq 1} \tilde{F}_b(x, y; \{s_i\}; \{t_i\}), \\ \tilde{F}_b(x, y; \{s_i\}; \{t_i\}) &= \frac{1}{b!} \sum_{\sum_i b_i = b} \sum_{\{n_i\}} \tilde{\mathcal{N}}_{h,k,l}(\{b_i\}, \{n_i\}) x^{h-2} y^k \prod_{i \geq 0} s_i^{b_i} t_i^{n_i}, \end{aligned} \quad (4.1)$$

and

$$\begin{aligned}\tilde{G}(x, y; \{s_i\}; \{q_i\}) &= \sum_{b \geq 1} \tilde{G}_b(x, y; \{s_i\}; \{q_i\}), \\ \tilde{G}_b(x, y; \{s_i\}; \{q_i\}) &= \frac{1}{b!} \sum_{\sum_i b_i = b} \sum_{\{p_i\}} \tilde{\mathcal{N}}_{h,k}(\{b_i\}, \{p_i\}) x^{h-2} y^k \prod_{i \geq 0} s_i^{b_i} \prod_{i \geq 1} q_i^{p_i}.\end{aligned}\tag{4.2}$$

Generating functions of connected and disconnected partial chord diagrams are related by

$$\tilde{Z}^P(x, y; \{s_i\}; \{t_i\}) = \exp \left[\tilde{F}(x, y; \{s_i\}; \{t_i\}) \right],\tag{4.3}$$

$$\tilde{Z}^L(x, y; \{s_i\}; \{q_i\}) = \exp \left[\tilde{G}(x, y; \{s_i\}; \{q_i\}) \right].\tag{4.4}$$

Furthermore, we introduce generating functions of non-oriented partial chord diagrams labeled by the boundary length and point spectrum.

Definition 4.2. Let $\tilde{\mathcal{N}}_{h,k,l}(\{b_i\}, \{n_i\})$ denote the number of connected orientable and non-orientable partial chord diagrams of type $\{h, k, l; \{b_i\}; \{n_i\}\}$ with the boundary length and point spectrum n_i . We define the generating functions

$$\begin{aligned}\tilde{\mathcal{F}}(x, y; \{s_i\}; \{u_i\}) &= \sum_{b \geq 1} \tilde{\mathcal{F}}_b(x, y; \{s_i\}; \{u_i\}), \\ \tilde{\mathcal{F}}_b(x, y; \{s_i\}; \{u_i\}) &= \frac{1}{b!} \sum_{\sum_i b_i = b} \sum_{\{n_i\}} \tilde{\mathcal{N}}_{h,k,l}(\{b_i\}, \{n_i\}) x^{h-2} y^k \prod_{i \geq 0} s_i^{b_i} \prod_{K \geq 1} \prod_{\{i_L\}_{L=1}^K} u_i^{n_i}.\end{aligned}\tag{4.5}$$

As usual, generating functions of connected and disconnected partial chord diagrams are related by

$$\tilde{\mathcal{Z}}(x, y; \{s_i\}; \{u_i\}) = \exp \left[\tilde{\mathcal{F}}(x, y; \{s_i\}; \{u_i\}) \right].\tag{4.6}$$

Non-oriented analogue of partial chord diagrams and Wick contractions.

A non-oriented partial chord diagram is a partial chord diagrams with each chord decorated by a binary variable, which indicates if it is twisted or not. Such non-oriented partial chord diagrams are enumerated by real symmetric⁹ matrix integrals. The Gaussian average $\langle \mathcal{O}(M) \rangle_N^{\tilde{G}}$ over the space $\mathcal{H}_N(\mathbb{R})$ of real symmetric matrices is defined by

$$\langle \mathcal{O}(M) \rangle_N^{\tilde{G}} = \frac{1}{\text{Vol}_N(\mathbb{R})} \int_{\mathcal{H}_N(\mathbb{R})} dM \mathcal{O}(M) e^{-N \text{Tr} \frac{M^2}{4}},\tag{4.7}$$

where

$$\text{Vol}_N(\mathbb{R}) = \int_{\mathcal{H}_N(\mathbb{R})} dM e^{-N \text{Tr} \frac{M^2}{4}} = N^{N(N+1)/2} \text{Vol}(\mathcal{H}_N(\mathbb{R})),\tag{4.8}$$

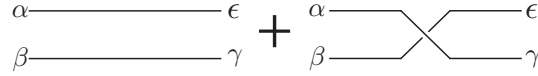
For the choice of $\mathcal{O}(M) = M_{\alpha\beta} M_{\gamma\epsilon}$ ($\alpha, \beta, \gamma, \epsilon = 1, \dots, N$), the Wick contraction is defined as

$$\overline{M_{\alpha\beta} M_{\gamma\epsilon}} := \langle M_{\alpha\beta} M_{\gamma\epsilon} \rangle_N^{\tilde{G}} = \frac{1}{N} (\delta_{\alpha\epsilon} \delta_{\beta\gamma} + \delta_{\alpha\gamma} \delta_{\beta\epsilon}).\tag{4.9}$$

⁹ The Gaussian matrix integral over the space of real symmetric matrix is also referred to as the *Gaussian orthogonal ensemble* [21, 35].

This Wick contraction consists of two terms, which encode the corresponding fat-graph as follows. The first term $\frac{1}{N}\delta_{\alpha\epsilon}\delta_{\beta\gamma}$ is the same as in the Hermitian matrix integral (2.5), and it can be identified with an untwisted band in the two dimensional surface Σ_c associated to the partial chord diagram c . The second term $\frac{1}{N}\delta_{\alpha\gamma}\delta_{\beta\epsilon}$ in (4.9) relates opposite matrix indices compared to the first term and can be identified with the twisted band in Σ_c , see Figure 14. Hence, for the real symmetric Gaussian average, the correspondence rules **C4**, **P5**, **L5** in Section 2 are replaced by the following rules [24, 54, 52, 26, 39, 23].

N5: The Wick contraction between $M_{\alpha_j\beta_j}$ and $M_{\alpha'_{j'}\beta'_{j'}}$ corresponds to a band or a twisted band connecting two chord ends. Each Wick contraction imposes either the constraint $\delta_{\alpha_j\beta'_{j'}}\delta_{\alpha'_{j'}\beta_j}$ or the constraint $\delta_{\alpha_j\alpha'_{j'}}\delta_{\beta_j\beta'_{j'}}$ for matrix indices assigned to edges of chord ends matched by Wick contractions.



$$\overline{M_{\alpha\beta}M_{\gamma\epsilon}} = \frac{1}{N}(\delta_{\alpha\epsilon}\delta_{\beta\gamma} + \delta_{\alpha\gamma}\delta_{\beta\epsilon})$$

FIGURE 14. Wick contraction and the untwisted / twisted bands.

In order to construct matrix models that enumerate non-oriented partial chord diagrams, we introduce two external real symmetric matrices Ω_P and Ω_L

$$\Omega_P = \Omega_P^T, \quad \Omega_L = \Omega_L^T,$$

which take account of the fact that boundary cycles of non-oriented partial chord diagrams are not endowed with a specific orientation. To model the index structure \mathbf{i} of the boundary length and point spectrum correctly, we assume these two matrices do not commute

$$[\Omega_P, \Omega_L] \neq 0.$$

Furthermore, we introduce corresponding generalized Miwa times

$$u_{(i_1, \dots, i_K)} = \frac{1}{N} \text{Tr} \left(\Omega_P^{i_1} \Omega_L^{-1} \Omega_P^{i_2} \Omega_L^{-1} \dots \Omega_P^{i_K} \Omega_L^{-1} \right), \quad (4.10)$$

which are invariant under the symmetry

$$u_{(i_1, \dots, i_K)} = u_{(i_K, i_{K-1}, \dots, i_1)}.$$

This assignment implies the bijective correspondence (analogous to the orientable case discussed earlier) between non-oriented partial chord diagrams and Wick contractions, which is summarized in Table 2.

Using this correspondence, generating functions $\tilde{Z}^P(x, y; \{s_i\}; \{r_i\})$, $\tilde{Z}^L(x, y; \{s_i\}; \{q_i\})$, and $\tilde{\mathcal{Z}}(x, y; \{s_i\}; \{u_i\})$ can be re-expressed in terms of matrix integrals. Repeating the same combinatorial arguments as for the orientable case in Section 2, we obtain the following three theorems.

TABLE 2. The correspondence between partial chord diagrams and operator products in the real symmetric matrix integral.

Partial chord diagram	Gaussian average
A chord end on a backbone	$\Omega_L^{-1}M$
A marked point on a backbone	Ω_P
An underside of a backbone	$N\Omega_L^{-1}$
A backbone	$N\text{Tr}(\Omega_P^{\alpha_1}\Omega_L^{-1}\Omega_P^{\alpha_2}\Omega_L^{-1}\dots\Omega_P^{\alpha_K}\Omega_L^{-1})$
A Chord	A Wick contraction \overline{MM}

Theorem 4.3. Let $\tilde{Z}_N^P(y; \{s_i\}; \{r_i\})$ be the real symmetric matrix integral with the external symmetric matrix Ω_P of rank N

$$\begin{aligned} \tilde{Z}_N^P(y; \{s_i\}; \{r_i\}) &= \\ &= \frac{1}{\text{Vol}_N(\mathbb{R})} \int_{\mathcal{H}_N(\mathbb{R})} dM \exp \left[-N\text{Tr} \left(\frac{M^2}{4} - \sum_{i \geq 0} s_i y^{i/2} (M + y^{-1/2} \Omega_P)^i \right) \right], \end{aligned} \quad (4.11)$$

where r_i are reverse Miwa times

$$r_i = \frac{1}{N} \text{Tr} \Omega_P^i. \quad (4.12)$$

This matrix integral agrees with the generating function (4.3)

$$\tilde{Z}_N^P(y; \{s_i\}; \{r_i\}) = \tilde{Z}^P(N^{-1}, y; \{s_i\}, t_0 = 1, \{t_i = r_i\}_{i \geq 1}). \quad (4.13)$$

The t_0 -dependence can be implemented by the following rescaling of parameters

$$\tilde{Z}_{t_0 N}^P(t_0 y; \{t_0^{-1} s_i\}; \{t_0^{-1} t_i\}) = \tilde{Z}^P(N^{-1}, y; \{s_i\}; \{t_i = r_i\}). \quad (4.14)$$

Theorem 4.4. Let $\tilde{Z}_N^L(y; \{s_i\}; \{q_i\})$ be the real symmetric matrix integral with the external invertible symmetric matrix Ω_L of rank N

$$\begin{aligned} \tilde{Z}_N^L(y; \{s_i\}; \{q_i\}) &= \\ &= \frac{1}{\text{Vol}_N(\mathbb{R})} \int_{\mathcal{H}_N(\mathbb{R})} dM \exp \left[-N\text{Tr} \left(\frac{M^2}{4} - \sum_{i \geq 0} s_i y^{i/2} (\Omega_L^{-1} M)^i \Omega_L^{-1} \right) \right], \end{aligned} \quad (4.15)$$

where q_i are Miwa times

$$q_i = \frac{1}{N} \text{Tr} \Omega_L^{-i}. \quad (4.16)$$

This matrix integral agrees with the generating function (4.4)

$$\tilde{Z}_N^L(y; \{s_i\}; \{q_i\}) = \tilde{Z}^L(N^{-1}, y; \{s_i\}; \{q_i\}). \quad (4.17)$$

As considered in (2.26) and Subsection 3.2, the specialization $s_i = s$ of the matrix integral (4.15) gives the following reduced model

$$\begin{aligned} \tilde{Z}_N^L(y; s; \{q_i\}) &= \tilde{Z}_N^L(y; \{s_i = s\}; \{q_i\}) = \\ &= \frac{1}{\text{Vol}_N(\mathbb{R})} \int_{\mathcal{H}_N(\mathbb{R})} dM \exp \left[-N\text{Tr} \left(\frac{M^2}{4} + \frac{s}{y^{1/2} M - \Omega_L} \right) \right]. \end{aligned} \quad (4.18)$$

The cut-and-join equation that follows from this reduced model is derived in the next subsection.

Theorem 4.5. *Let $\tilde{\mathcal{Z}}_N(y; \{s_i\}; \{u_i\})$ be the real symmetric matrix integral with the external invertible symmetric matrices Ω_P and Ω_L of rank N*

$$\begin{aligned} \tilde{\mathcal{Z}}_N(y; \{s_i\}; \{u_i\}) &= \\ &= \frac{1}{\text{Vol}_N(\mathbb{R})} \int_{\mathcal{H}_N(\mathbb{R})} dM \exp \left[-N \text{Tr} \left(\frac{M^2}{4} - \sum_{i \geq 0} s_i (y^{1/2} \Omega_L^{-1} M + \Omega_P)^i \Omega_L^{-1} \right) \right], \end{aligned} \quad (4.19)$$

and u_i be the generalized Miwa times defined in (4.10). This matrix integral agrees with the generating function (4.6)

$$\tilde{\mathcal{Z}}_N(y; \{s_i\}; \{u_i\}) = \tilde{\mathcal{Z}}(N^{-1}, y; \{s_i\}; \{u_i\}). \quad (4.20)$$

4.2. Non-oriented analogues of cut-and-join equations. We derive now non-oriented analogues of cut-and-join equations discussed in Section 3. Analogously to the Hermitian matrix integral in (3.1), we introduce the following matrix integral.

Definition 4.6. Let $U = U^T$ and $V = V^T$ be rank N invertible symmetric matrices. We define a formal real symmetric matrix integral with parameters $y, \{g_i\}_{i=-\infty}^{+\infty}$ as follows

$$\begin{aligned} \tilde{\mathcal{Z}}_N(y; \{g_i\}; U; V) &= \\ &= \frac{1}{\text{Vol}_N(\mathbb{R})} \int_{\mathcal{H}_N(\mathbb{R})} dM \exp \left[-N \text{Tr} \left(\frac{1}{4} M^2 - \sum_{i \in \mathbb{Z}} g_i (y^{1/2} V^{-1} M + U)^i V^{-1} \right) \right]. \end{aligned} \quad (4.21)$$

The matrix integrals discussed in the previous subsection follow from this matrix integral by specializations

$$\tilde{\mathcal{Z}}_N^P(y; \{s_i\}; \{r_i\}) : \quad g_{i < 0} = 0, \quad g_{i \geq 0} = s_i, \quad U = \Omega_P, \quad V = I_N, \quad (4.22)$$

$$\tilde{\mathcal{Z}}_N^L(y; \{s_i\}; \{q_i\}) : \quad g_{i < 0} = 0, \quad g_{i \geq 0} = s_i, \quad U = 0, \quad V = \Omega_L, \quad (4.23)$$

$$\tilde{\mathcal{Z}}_N^L(y; s; \{q_i\}) : \quad g_{i \neq -1} = 0, \quad g_{-1} = -s, \quad U = \Omega_L, \quad V = -I_N, \quad (4.24)$$

$$\tilde{\mathcal{Z}}_N(y; \{s_i\}; \{u_i\}) : \quad g_{i < 0} = 0, \quad g_{i \geq 0} = s_i, \quad U = \Omega_P, \quad V = \Omega_L, \quad (4.25)$$

where I_N is the rank N identity matrix.

In Appendix A we prove the following proposition.

Proposition 4.7. *The matrix integral $\tilde{\mathcal{Z}}_N(y; \{g_i\}; U; V)$ in (4.21) obeys the partial differential equation*

$$\left[\frac{\partial}{\partial y} - \frac{1}{4N} \text{Tr}(V^{-1})^T \frac{\partial}{\partial A} (V^{-1})^T \frac{\partial}{\partial A} \right] \tilde{\mathcal{Z}}_N(y; \{g_i\}; U; V) = 0, \quad (4.26)$$

where A is a matrix such that

$$U = A + A^T.$$

From this proposition and by the specializations (4.22), (4.24), and (4.25) we find partial differential equations for the corresponding matrix integrals. For the specialization (4.23), because of $U = 0$ (and thus $A = 0$), the partial differential equation (4.26) cannot be reduced to a partial differential equation.

Corollary 4.8. *The matrix integral $\tilde{Z}_N^P(y; \{s_i\}; \{r_i\})$ in (4.11), $\tilde{Z}_N^L(y; s; \{q_i\})$ in (4.18) and $\tilde{Z}_N(y; \{s_i\}; \{u_i\})$ in (4.19) obey partial differential equations*

$$\begin{aligned} \left[\frac{\partial}{\partial y} - \frac{1}{4N} \text{Tr} \frac{\partial^2}{\partial \Lambda_P^2} \right] \tilde{Z}_N^P(y; \{s_i\}; \{r_i\}) &= 0, \\ \left[\frac{\partial}{\partial y} - \frac{1}{4N} \text{Tr} \frac{\partial^2}{\partial \Lambda_L^2} \right] \tilde{Z}_N^L(y; s; \{q_i\}) &= 0, \\ \left[\frac{\partial}{\partial y} - \frac{1}{4N} \text{Tr} (\Omega_L^{-1})^T \frac{\partial}{\partial \Lambda_P} (\Omega_L^{-1})^T \frac{\partial}{\partial \Lambda_P} \right] \tilde{Z}_N(y; \{s_i\}; \{u_i\}) &= 0, \end{aligned} \quad (4.27)$$

where Λ_P and Λ_L are matrices satisfying

$$\Omega_P = \Lambda_P + \Lambda_P^T, \quad \Omega_L = \Lambda_L + \Lambda_L^T.$$

From this corollary we obtain non-oriented analogues of cut-and-join equations, by rewriting the derivatives with respect to the external matrices Λ_P and Λ_L in Corollary 4.8 in terms of Miwa times r_i in (4.12), q_i in (4.16), and u_i in (4.10) as follows.

Lemma 4.9. *Let L_1 , K_1 , M_1 , and M_2^\vee denote differential operators*

$$L_1 = \frac{1}{2} \sum_{i \geq 1} i(i+1) r_i \frac{\partial}{\partial r_{i+2}}, \quad (4.28)$$

$$K_1 = \frac{1}{2} \sum_{i \geq 3} (i-2)(i-1) q_i \frac{\partial}{\partial q_{i-2}}, \quad (4.29)$$

$$\begin{aligned} M_1 &= \frac{1}{2} \sum_{K \geq 1} \sum_{\{i_1, \dots, i_K\}} \sum_{1 \leq I \neq M \leq K} \sum_{\ell=0}^{i_I-1} \sum_{m=0}^{i_M-1} \\ &\quad u(m, i_{M-1}, i_{M-2}, \dots, i_{I+1}, i_I - \ell - 1, i_M - m - 1, i_{M+1}, \dots, i_{I-1}, \ell) \frac{\partial}{\partial u_{(i_1, \dots, i_K)}} \\ &\quad + \sum_{K \geq 1} \sum_{\{i_1, \dots, i_K\}} \sum_{L=1}^K \sum_{\ell+m \leq i_L-2} u(\ell, i_I - \ell - m - 2, m, i_{I+1}, \dots, i_{I-1}) \frac{\partial}{\partial u_{(i_1, \dots, i_K)}}, \end{aligned} \quad (4.30)$$

and

$$\begin{aligned} M_2^\vee &= \frac{1}{2} \sum_{K, L \geq 1} \sum_{\{i_1, \dots, i_K\}} \sum_{\{j_1, \dots, j_L\}} \sum_{I=1}^K \sum_{J=1}^L \sum_{\ell=0}^{i_I-1} \sum_{m=0}^{j_J-1} \\ &\quad u(\ell, i_{I-1}, \dots, i_{I+1}, i_I - \ell - 1, j_J - m - 1, j_{J+1}, \dots, j_{J-1}, m) \frac{\partial^2}{\partial u_{(i_1, \dots, i_K)} \partial u_{(j_1, \dots, j_L)}}. \end{aligned} \quad (4.31)$$

Then the derivatives with respect to Λ_P and Λ_L in Corollary 4.8 are rewritten as

$$\begin{aligned} \frac{1}{4N} \text{Tr} \frac{\partial^2}{\partial \Lambda_P^2} f(\{r_i\}) &= \left(L_0 + \frac{1}{N} L_1 + \frac{2}{N^2} L_2 \right) f(\{r_i\}), \\ \frac{1}{4N} \text{Tr} \frac{\partial^2}{\partial \Lambda_L^2} g(\{q_i\}) &= \left(K_0 + \frac{1}{N} K_1 + \frac{2}{N^2} K_2 \right) g(\{q_i\}), \\ \frac{1}{4N} \text{Tr} \left[(\Omega_L^{-1})^T \frac{\partial}{\partial \Lambda_P} (\Omega_L^{-1})^T \frac{\partial}{\partial \Lambda_P} \right] h(\{u_i\}) \\ &= \left(M_0 + \frac{1}{N} M_1 + \frac{1}{N^2} (M_2 + M_2^\vee) \right) h(\{u_i\}), \end{aligned} \quad (4.32)$$

where $f(\{r_i\})$, $g(\{q_i\})$, and $h(\{u_i\})$ are functions of Miwa times r_i , q_i , and u_i , respectively. Here $L_{0,2}$, $K_{0,2}$, and $M_{0,2}$ are defined in (3.7), (3.16), and (3.22), respectively.

The proof of this lemma is given in Appendix B. By combining Corollary 4.8 with Lemma 4.9 one arrives at the following theorem.

Theorem 4.10. *The matrix integrals $\tilde{Z}_N^P(y; \{s_i\}; \{r_i\})$ in (4.11), $\tilde{Z}_N^L(y; s; \{q_i\})$ in (4.18), and $\tilde{Z}_N(y; \{s_i\}; \{u_i\})$ in (4.19) obey the cut-and-join equations*

$$\begin{aligned} \frac{\partial}{\partial y} \tilde{Z}_N^P(y; \{s_i\}; \{r_i\}) &= \tilde{\mathcal{L}} \tilde{Z}_N^P(y; \{s_i\}; \{r_i\}), \\ \frac{\partial}{\partial y} \tilde{Z}_N^L(y; s; \{q_i\}) &= \tilde{\mathcal{K}} \tilde{Z}_N^L(y; s; \{q_i\}), \\ \frac{\partial}{\partial y} \tilde{Z}_N(y; \{s_i\}; \{u_i\}) &= \tilde{\mathcal{M}} \tilde{Z}_N(y; \{s_i\}; \{u_i\}), \end{aligned} \quad (4.33)$$

where

$$\begin{aligned} \tilde{\mathcal{L}} &= L_0 + \frac{1}{N} L_1 + \frac{2}{N^2} L_2, \\ \tilde{\mathcal{K}} &= K_0 + \frac{1}{N} K_1 + \frac{2}{N^2} K_2, \\ \tilde{\mathcal{M}} &= M_0 + \frac{1}{N} M_1 + \frac{1}{N^2} (M_2 + M_2^\vee). \end{aligned}$$

Assuming certain initial conditions at $y = 0$, one can iteratively determine the above matrix integrals by solving the cut-and-join equations

$$\begin{aligned} \tilde{Z}_N^P(y; \{s_i\}; \{r_i\}) &= e^{y\tilde{\mathcal{L}}} \tilde{Z}_N^P(y=0; \{s_i\}; \{r_i\}) = e^{y\tilde{\mathcal{L}}} e^{N^2 \sum_{i \geq 0} s_i r_i}, \\ \tilde{Z}_N^L(y; s; \{q_i\}) &= e^{y\tilde{\mathcal{K}}} \tilde{Z}_N^L(y=0, s; \{q_i\}) = e^{y\tilde{\mathcal{K}}} e^{N^2 s q_1}, \\ \tilde{Z}_N(y; \{s_i\}; \{u_i\}) &= e^{y\tilde{\mathcal{M}}} \tilde{Z}_N(y=0; \{s_i\}; \{u_i\}) = e^{y\tilde{\mathcal{M}}} e^{-N^2 \sum_{i \geq 0} s_i u_{(i)}}. \end{aligned} \quad (4.34)$$

The cut-and-join equations (4.33) agree with those of [2, 7]. Finally, from Theorem 4.10 we find non-oriented analogues of cut-and-join equations for 1-backbone generating functions.

Corollary 4.11. *The 1-backbone generating function $\tilde{\mathcal{F}}_1(x, y; \{s_i\}; \{u_i\})$ obtained by picking up the $\mathcal{O}(s_i^1)$ term in $\tilde{Z}_N(y; \{s_i\}; \{u_i\})$ is given by the following matrix*

integral

$$\begin{aligned} \tilde{\mathcal{F}}_1(N^{-1}, y; \{s_i\}; \{u_{\mathbf{i}}\}) &= \\ &= \frac{1}{\text{Vol}_N(\mathbb{R})} \int_{\mathcal{H}_N(\mathbb{R})} dM \, e^{-N \text{Tr} \frac{M^2}{4}} N \sum_{i \geq 0} s_i \text{Tr}(y^{1/2} \Omega_L^{-1} M + \Omega_P)^i \Omega_L^{-1}, \end{aligned} \quad (4.35)$$

and it obeys the cut-and-join equation

$$\frac{\partial}{\partial y} \tilde{\mathcal{F}}_1(x, y; \{s_i\}; \{u_{\mathbf{i}}\}) = \widetilde{\mathcal{M}} \tilde{\mathcal{F}}_1(x, y; \{s_i\}; \{u_{\mathbf{i}}\}), \quad (4.36)$$

where $\widetilde{\mathcal{M}} = M_0 + xM_1 + x^2(M_2 + M_2^\vee)$. The solution is iteratively determined by

$$\tilde{\mathcal{F}}_1(x, y; \{s_i\}; \{u_{\mathbf{i}}\}) = e^{y\widetilde{\mathcal{M}}} \tilde{\mathcal{F}}_1(x, y=0; \{s_i\}; \{u_{\mathbf{i}}\}) = e^{y\widetilde{\mathcal{M}}} \left(x^{-2} \sum_{i \geq 0} s_i u_{(i)} \right). \quad (4.37)$$

APPENDIX A. PROOF OF PROPOSITION 4.7

In this appendix we prove the Proposition 4.7, which states that the matrix integral

$$\begin{aligned} \tilde{Z}_N(y; \{g_i\}; U; V) &= \\ &= \frac{1}{\text{Vol}_N(\mathbb{R})} \int_{\mathcal{H}_N(\mathbb{R})} dM \exp \left[-N \text{Tr} \left(\frac{1}{4} M^2 - \sum_{i \in \mathbb{Z}} g_i (y^{1/2} V^{-1} M + U)^i V^{-1} \right) \right], \end{aligned}$$

obeys the partial differential equation

$$\left[\frac{\partial}{\partial y} - \frac{1}{4N} \text{Tr}(V^{-1})^T \frac{\partial}{\partial A} (V^{-1})^T \frac{\partial}{\partial A} \right] \tilde{Z}_N(y; \{g_i\}; U; V) = 0, \quad (\text{A.1})$$

where A is a matrix that satisfies $U = A + A^T$.

Proof. In order to differentiate the matrix integral $\tilde{Z}_N(y; \{g_i\}; U; V)$ with respect to A we use the identities

$$\begin{aligned} \frac{\partial U_{\alpha\beta}}{\partial A_{\gamma\epsilon}} &= \delta_{\alpha\gamma} \delta_{\beta\epsilon} + \delta_{\alpha\epsilon} \delta_{\beta\gamma}, \\ \frac{\partial (y^{1/2} V^{-1} X)_{\alpha\beta}^{-1}}{\partial A_{\gamma\epsilon}} &= -(y^{1/2} V^{-1} X)_{\alpha\gamma}^{-1} (y^{1/2} V^{-1} X)_{\beta\epsilon}^{-1} - (y^{1/2} V^{-1} X)_{\alpha\epsilon}^{-1} (y^{1/2} V^{-1} X)_{\beta\gamma}^{-1}, \end{aligned}$$

where $X = M + y^{-1/2} V U$. Using this shifted variable X one obtains

$$\begin{aligned} \frac{1}{2N} \frac{\partial}{\partial A_{\alpha\beta}} \tilde{Z}_N(y; \{g_i\}; U; V) &= \left\langle \sum_{i=0}^{\infty} y^{(i-1)/2} g_i \sum_{j=0}^{i-1} ((V^{-1} X)^j V^{-1} (V^{-1} X)^{i-j-1})_{\alpha\beta} \right. \\ &\quad \left. - \sum_{i=1}^{\infty} y^{-(i+1)/2} g_{-i} \sum_{j=0}^{i-1} ((V^{-1} X)^{-j-1} V^{-1} (V^{-1} X)^{-i+j})_{\alpha\beta} \right\rangle_{\mathbb{R}}, \end{aligned}$$

where $\langle \cdots \rangle_{\mathbb{R}}$ denotes the unnormalized average

$$\langle \mathcal{O}(X) \rangle_{\mathbb{R}} = \int_{\tilde{\mathcal{H}}_N(\mathbb{R})} dX \mathcal{O}(X) \exp \left[-N \text{Tr} \left(\frac{1}{4} (X - y^{-1/2} V U)^2 - \sum_{i \in \mathbb{Z}} y^{i/2} g_i (V^{-1} X)^i V^{-1} \right) \right].$$

Here $\tilde{\mathcal{H}}_N(\mathbb{R})$ is the space of shifted matrices $X = M + y^{-1/2} V U$ with $M \in \mathcal{H}_N(\mathbb{R})$. It follows that

$$\begin{aligned} \frac{1}{2N^2} \text{Tr}(V^{-1})^T \frac{\partial}{\partial A} (V^{-1})^T \frac{\partial}{\partial A} \tilde{Z}_N(y; \{g_i\}; U; V) &= \\ &= \left\langle \sum_{i=0}^{\infty} y^{-1/2} g_i \sum_{j=0}^{i-1} \text{Tr}(X - y^{-1/2} V U) V^{-1} (y^{1/2} V^{-1} X)^j V^{-1} (y^{1/2} V^{-1} X)^{i-j-1} \right. \\ &\quad \left. - \sum_{i=1}^{\infty} y^{-1/2} g_{-i} \sum_{j=0}^{i-1} \text{Tr}(X - y^{-1/2} V U) V^{-1} (y^{1/2} V^{-1} X)^{-j-1} V^{-1} (y^{1/2} V^{-1} X)^{-i+j} \right\rangle_{\mathbb{R}}. \end{aligned} \quad (\text{A.2})$$

On the other hand, by differentiating the matrix integral $\tilde{Z}_N(y; \{g_i\}; U; V)$ with respect to y one obtains the same expression as (A.2) times $N/2$, from which the partial differential equation (A.1) is obtained. \square

APPENDIX B. PROOF OF LEMMA 4.9

In this appendix we prove the Lemma 4.9, which states that for functions $f(\{r_i\})$, $g(\{q_i\})$, and $h(\{u_i\})$ of Miwa times r_i in (4.12), q_i in (4.16), and u_i in (4.10), we find

$$\frac{1}{4N} \text{Tr} \frac{\partial^2}{\partial \Lambda_P^2} f(\{r_i\}) = \left(L_0 + \frac{1}{N} L_1 + \frac{2}{N^2} L_2 \right) f(\{r_i\}), \quad (\text{B.1})$$

$$\frac{1}{4N} \text{Tr} \frac{\partial^2}{\partial \Lambda_L^2} g(\{q_i\}) = \left(K_0 + \frac{1}{N} K_1 + \frac{2}{N^2} K_2 \right) g(\{q_i\}), \quad (\text{B.2})$$

$$\begin{aligned} \frac{1}{4N} \text{Tr} \left[(\Omega_L^{-1})^T \frac{\partial}{\partial \Lambda_P} (\Omega_L^{-1})^T \frac{\partial}{\partial \Lambda_P} \right] h(\{u_i\}) \\ = \left(M_0 + \frac{1}{N} M_1 + \frac{1}{N^2} (M_2 + M_2^\vee) \right) h(\{u_i\}), \end{aligned} \quad (\text{B.3})$$

where $L_{0,1,2}$, $K_{0,1,2}$, $M_{0,1,2}$, and M_2^\vee are defined in (3.7), (3.16), (3.22), and in Lemma 4.9. Here the matrices Λ_P and Λ_L satisfy $\Omega_P = \Lambda_P + \Lambda_P^T$ and $\Omega_L = \Lambda_L + \Lambda_L^T$. **Proof.** First we prove (B.1). Consider the derivative $\partial/\partial \Lambda_P$ of the reverse Miwa time r_i

$$\frac{\partial r_i}{\partial \Lambda_{P\beta\alpha}} = \frac{2i}{N} \Omega_{P\alpha\beta}^{i-1}, \quad \text{Tr} \frac{\partial^2 r_i}{\partial \Lambda_P^2} = 2Ni \sum_{j=1}^{i-1} r_{j-1} r_{i-j-1} + 2i(i-1) r_{i-2}.$$

Using these relations the left hand side of (B.1) is rewritten as

$$\begin{aligned} \frac{1}{4N} \text{Tr} \frac{\partial^2}{\partial \Lambda_P^2} f(\{r_i\}) &= \frac{1}{4N} \sum_{i \geq 1} \text{Tr} \frac{\partial^2 r_i}{\partial \Lambda_P^2} \frac{\partial f(\{r_i\})}{\partial r_i} + \frac{1}{4N} \sum_{i,j \geq 1} \text{Tr} \frac{\partial r_i}{\partial \Lambda_P} \frac{\partial r_j}{\partial \Lambda_P} \frac{\partial^2 f(\{r_i\})}{\partial r_i \partial r_j} \\ &= \frac{1}{2} \sum_{i \geq 2} \sum_{j=1}^{i-1} i r_{j-1} r_{i-j-1} \frac{\partial f(\{r_i\})}{\partial r_i} + \frac{1}{2N} \sum_{i \geq 2} i(i-1) r_{i-2} \frac{\partial f(\{r_i\})}{\partial r_i} \\ &\quad + \frac{1}{N^2} \sum_{i,j \geq 1} i j r_{i+j-2} \frac{\partial}{\partial r_i} \frac{\partial}{\partial r_j} f(\{r_i\}). \end{aligned}$$

This agrees with the right hand side of (B.1).

Second, we prove (B.2). Using the identity

$$\frac{\partial \Omega_{L\gamma\epsilon}^{-1}}{\partial \Lambda_{L\alpha\beta}} = -\Omega_{L\beta\epsilon}^{-1} \Omega_{L\gamma\alpha}^{-1} - \Omega_{L\alpha\epsilon}^{-1} \Omega_{L\gamma\beta}^{-1},$$

one finds that

$$\frac{\partial q_i}{\partial \Lambda_{L\alpha\beta}} = -2 \frac{i}{N} \Omega_{L\beta\alpha}^{-i-1}, \quad \text{Tr} \frac{\partial^2}{\partial \Lambda_L^2} q_i = 2i(i+1) q_{i+2} + 2iN \sum_{j=0}^i q_{i+1} q_{j+1}.$$

Then the left hand side of (B.2) yields

$$\begin{aligned} \frac{1}{4N} \text{Tr} \frac{\partial^2}{\partial \Lambda_L^2} g(\{q_i\}) &= \frac{1}{2} \sum_{i \geq 1} \sum_{j=0}^i i q_{i+1} q_{j+1} \frac{\partial g(\{q_i\})}{\partial q_i} + \frac{1}{2N} \sum_{i \geq 1} i(i+1) q_{i+2} \frac{\partial g(\{q_i\})}{\partial q_i} \\ &\quad + \frac{1}{N^2} \sum_{i,j \geq 1} i j q_{i+j+2} \frac{\partial^2 g(\{q_i\})}{\partial q_i \partial q_j}. \end{aligned}$$

This agrees with the right hand side of (B.2).

Finally we prove (B.3). Using the chain rule, the derivative action on the left hand side of (B.3) is written as

$$\begin{aligned}
& \text{Tr} \left[(\Omega_L^{-1})^T \frac{\partial}{\partial \Lambda_P} (\Omega_L^{-1})^T \frac{\partial}{\partial \Lambda_P} \right] h(\{u_{\mathbf{i}}\}) = \\
& = \sum_{K \geq 1} \sum_{\{i_1, \dots, i_K\}} \text{Tr} \left[(\Omega_L^{-1})^T \frac{\partial}{\partial \Lambda_P} (\Omega_L^{-1})^T \frac{\partial}{\partial \Lambda_P} u_{(i_1, \dots, i_K)} \right] \frac{\partial}{\partial u_{(i_1, \dots, i_K)}} h(\{u_{\mathbf{i}}\}) \\
& + \sum_{K, L \geq 1} \sum_{\{i_1, \dots, i_K\}} \sum_{\{j_1, \dots, j_L\}} \text{Tr} \left[(\Omega_L^{-1})^T \frac{\partial}{\partial \Lambda_P} u_{(i_1, \dots, i_K)} (\Omega_L^{-1})^T \frac{\partial}{\partial \Lambda_P} u_{(j_1, \dots, j_L)} \right] \\
& \quad \times \frac{\partial^2}{\partial u_{(i_1, \dots, i_K)} \partial u_{(j_1, \dots, j_L)}} h(\{u_{\mathbf{i}}\}).
\end{aligned}$$

Each of the coefficients yields

$$\begin{aligned}
& \text{Tr} \left[(\Omega_L^{-1})^T \frac{\partial}{\partial \Lambda_P} (\Omega_L^{-1})^T \frac{\partial}{\partial \Lambda_P} u_{(i_1, \dots, i_K)} \right] = \\
& = 2 \sum_{1 \leq I \neq M \leq K}^K \sum_{\ell=0}^{i_I-1} \sum_{m=0}^{i_M-1} \frac{1}{N} \left(\text{Tr}(\Omega_P^{i_I-\ell-1} \Omega_L^{-1} \Omega_P^{i_I+1} \Omega_L^{-1} \dots \Omega_P^{i_M-1} \Omega_L^{-1} \Omega_P^m \Omega_L^{-1}) \right. \\
& \quad \times \text{Tr}(\Omega_P^{i_M-m-1} \Omega_L^{-1} \Omega_P^{i_M+1} \Omega_L^{-1} \dots \Omega_P^{i_I-1} \Omega_L^{-1} \Omega_P^\ell \Omega_L^{-1}) \\
& \quad + \text{Tr}(\Omega_P^m \Omega_L^{-1} \Omega_P^{i_M-1} \Omega_L^{-1} \Omega_P^{i_M-2} \Omega_L^{-1} \dots \Omega_P^{i_I+1} \Omega_L^{-1} \Omega_P^{i_I-\ell-1} \Omega_L^{-1}) \\
& \quad \cdot \Omega_P^{i_M-m-1} \Omega_L^{-1} \Omega_P^{i_M+1} \Omega_L^{-1} \Omega_P^{i_M+2} \Omega_L^{-1} \dots \Omega_P^{i_I-1} \Omega_L^{-1} \Omega_P^\ell \Omega_L^{-1} \Big) \\
& + 4 \sum_{I=1}^K \sum_{\ell+m \leq i_I-2} \left(\frac{1}{N} \text{Tr}(\Omega_P^\ell \Omega_L^{-1} \Omega_P^m \Omega_L^{-1} \Omega_P^{i_I+1} \Omega_L^{-1} \dots \Omega_P^{i_I-1} \Omega_L^{-1}) \text{Tr}(\Omega_P^{i_I-\ell-m-2} \Omega_L^{-1}) \right. \\
& \quad \left. + \text{Tr}(\Omega_P^\ell \Omega_L^{-1} \Omega_P^m \Omega_L^{-1} \Omega_P^{i_I-\ell-m-2} \Omega_L^{-1} \Omega_P^{i_I+1} \Omega_L^{-1} \dots \Omega_P^{i_I-1} \Omega_L^{-1}) \right) \\
& = 2 \sum_{1 \leq I \neq M \leq K} \sum_{\ell=0}^{i_I-1} \sum_{m=0}^{i_M-1} \left(N u_{(i_I-\ell-1, i_{I+1}, \dots, i_{M-1}, m)} u_{(i_M-m-1, i_{M+1}, \dots, i_{I-1}, \ell)} \right. \\
& \quad \left. + u_{(m, i_{M-1}, i_{M-2}, \dots, i_{I+1}, i_I-\ell-1, i_M-m-1, i_{M+1}, \dots, i_{I-1}, \ell)} \right) \\
& + 4 \sum_{I=0}^K \sum_{\ell+m \leq i_I-2} \left(N u_{(\ell, m, i_{I+1}, \dots, i_{I-1})} u_{(i_I-\ell-m-2)} + u_{(\ell, i_I-\ell-m-2, m, i_{I+1}, \dots, i_{I-1})} \right),
\end{aligned}$$

and

$$\begin{aligned}
& \text{Tr} \left[(\Omega_L^{-1})^T \frac{\partial}{\partial \Lambda_P} u_{(i_1, \dots, i_K)} (\Omega_L^{-1})^T \frac{\partial}{\partial \Lambda_P} u_{(j_1, \dots, j_L)} \right] = \\
&= \sum_{I=1}^K \sum_{J=1}^L \sum_{\ell=0}^{i_I-1} \sum_{m=0}^{j_J-1} \frac{2}{N^2} \left(\text{Tr} (\Omega_P^{i_I-\ell-1} \Omega_L^{-1} \Omega_P^{i_I+1} \Omega_L^{-1} \dots \Omega^{i_I-1} \Omega_L^{-1} \Omega_P^\ell \Omega_L^{-1} \right. \\
&\quad \cdot \Omega_P^{j_J-m-1} \Omega_L^{-1} \Omega_P^{j_J+1} \Omega_L^{-1} \dots \Omega^{j_J-1} \Omega_L^{-1} \Omega_P^m \Omega_L^{-1}) \\
&\quad + \text{Tr} (\Omega_P^\ell \Omega_L^{-1} \Omega_P^{i_I-1} \Omega_L^{-1} \dots \Omega^{i_I+1} \Omega_L^{-1} \Omega_P^{i_I-\ell-1} \Omega_L^{-1} \\
&\quad \cdot \Omega_P^{j_J-m-1} \Omega_L^{-1} \Omega_P^{j_J+1} \Omega_L^{-1} \dots \Omega^{j_J-1} \Omega_L^{-1} \Omega_P^m \Omega_L^{-1}) \Big) \\
&= \frac{2}{N} \sum_{I=1}^K \sum_{J=1}^L \sum_{\ell=0}^{i_I-1} \sum_{m=0}^{j_J-1} \left(u_{(i_I-\ell-1, i_{I+1}, \dots, i_{I-1}, \ell, j_J-m-1, j_{J+1}, \dots, j_{J-1}, m)} \right. \\
&\quad \left. + u_{(\ell, i_{I-1}, \dots, i_{I+1}, i_I-\ell-1, j_J-m-1, j_{J+1}, \dots, j_{J-1}, m)} \right).
\end{aligned}$$

Then one obtains the right hand side of (B.3). \square

REFERENCES

- [1] T. Akutsu, *Dynamic programming algorithms for RNA secondary structure prediction with pseudoknots*, Disc. Appl. Math. **104** (2000) 45–62.
- [2] N. V. Alexeev, J. E. Andersen, R. C. Penner, and P. Zograf, *Enumeration of Chord Diagrams on many intervals and their non-orientable analogs*, Adv. Math. **289** (2016) 1056–1081, arXiv:1307.0967 [math.CO].
- [3] J. E. Andersen, A. J. Bene, J. -B. Meilhan, and R. C. Penner, *Finite type invariants and fatgraphs*, Adv. Math. **225** (2010), 2117–2161.
- [4] J. E. Andersen, L. O. Chekhov, R. C. Penner, C. M. Reidys, and P. Sulkowski, *Topological recursion for chord diagrams, RNA complexes, and cells in moduli spaces*, Nucl. Phys. **B866** (2013) 414–443, arXiv:1205.0658 [hep-th].
- [5] J. E. Andersen, L. O. Chekhov, R. C. Penner, C. M. Reidys, and P. Sulkowski, *Enumeration of RNA complexes via random matrix theory*, Biochem. Soc. Trans. **41** (2013) 652–655, arXiv:1303.1326 [q-bio.QM].
- [6] J. E. Andersen, H. Fuji, M. Manabe, R. C. Penner, and P. Sulkowski, *Enumeration of chord diagrams via topological recursion and quantum curve techniques*, Preprint.
- [7] J. E. Andersen, H. Fuji, R. C. Penner, and C. M. Reidys, *The boundary length and point spectrum enumeration of partial chord diagrams via cut and join recursion*, Preprint.
- [8] J. E. Andersen, F. W. D. Huang, R. C. Penner, C. M. Reidys, *Topology of RNA-RNA interaction structures*, J. Comp. Biol. **19** (2012) 928–943, arXiv:1112.6194 [math.CO].
- [9] J. E. Andersen, J. Mattes, and N. Reshetikhin, *The Poisson Structure on the Moduli Space of Flat Connections and Chord Diagrams*, Topology **35** (1996) 1069–1083.
- [10] J. E. Andersen, J. Mattes, and N. Reshetikhin, *Quantization of the algebra of chord diagrams*, Math. Proc. Camb. Phil. Soc. **124** (1998) 451–467.
- [11] J. E. Andersen, R. C. Penner, C. M. Reidys, R. R. Wang, *Linear chord diagrams on two intervals*, arXiv:1010.5857 [math.CO].
- [12] J. E. Andersen, R. C. Penner, C. M. Reidys, M. S. Waterman, *Enumeration of linear chord diagrams*, J. Math. Biol. **67** (2013) 1261–78, arXiv:1010.5614 [math.CO].
- [13] M. Andronescu, V. Bereg, H. H. Hoos, and A. Condon, *RNA STRAND: The RNA Secondary Structure And Statistical Analysis Database*, BMC Bioinformatics, **9** (2008) 340.
- [14] D. Bar-Natan, *On the Vassiliev knot invariants*, Topology **34** (1995) 423–475.
- [15] D. Bessis, C. Itzykson, and J. B. Zuber, *Quantum field theory techniques in graphical enumeration*, Adv. Appl. Math. **1** (1980) 109–157.
- [16] R. Campoamor-Stursberg and V. O. Manturov, *Invariant tensor formulas via chord diagrams*, Jour. Math. Sci. **108** (2004) 3018–3029.

- [17] H. L. Chen, A. Condon, and H. Jabbari, *An $O(n^5)$ Algorithm for MFE Prediction of Kissing Hairpins and 4-Chains in Nucleic Acids*, J. Comput. Biol. **16** (2009) 803–815.
- [18] J. Courtiel, K. Yeats, *Terminal chords in connected chord diagrams*, arXiv:1603.08596 [math.CO].
- [19] R. Dijkgraaf, H. L. Verlinde and E. P. Verlinde, *Loop equations and Virasoro constraints in nonperturbative 2-D quantum gravity*, Nucl. Phys. B **348**, 435 (1991).
- [20] O. Dumitrescu, M. Mulase, B. Safnuk and A. Sorkin, *The spectral curve of the Eynard-Orantin recursion via the Laplace transform*, Contemp. Math. **593**, 263 (2013) [arXiv:1202.1159 [math.AG]].
- [21] F. J. Dyson, *The S matrix in quantum electrodynamics*, Phys. Rev. **75** (1949) 1736–1755.
- [22] M. Fukuma, H. Kawai and R. Nakayama, *Continuum Schwinger-dyson Equations and Universal Structures in Two-dimensional Quantum Gravity*, Int. J. Mod. Phys. A **6**, 1385 (1991).
- [23] S. Garoufalidis, and M. Marino, *Universality and asymptotics of graph counting problems in nonorientable surfaces*, Jour. Comb. Thor. **A117** (2010) 715–740, arXiv:0812.1195 [math.CO].
- [24] I. P. Goulden, J. L. Harer, and D. M. Jackson, *A geometric parametrization for the virtual Euler characteristics of the moduli spaces of real and complex algebraic curves*, Trans. Amer. Math. Soc. **353** (2001), no. 11, 4405–4427.
- [25] I. L. Hofacker, W. Fontana, P. F. Stadler, L. S. Bonhoffer, M. Tacker, and P. Schuster, *Fast folding and comparison of RNA secondary structures*, Monatsh. Chem. **125** (1994) 167–188.
- [26] R. A. Janik, M. A. Nowak, G. Papp, and Z. Ismail, *Green’s functions in non-hermitian random matrix models*, Physica **E9** (2001) 456–462, arXiv: cond-mat/9909085.
- [27] M. Kazarian, and P. Zograf, *Virasoro constraints and topological recursion for Grothendieck’s dessin counting*, Lett. Math. Phys. **105** (2015) 1057–1084, arXiv:1406.5976 [math.CO].
- [28] D. A. M. Konings, and R. R. Gutell *A comparison of thermodynamic foldings with comparatively derived structures of 16s and 16s-like r RNAs*, RNA **1** (1995) 559–574.
- [29] M. Kontsevich, Funk. Anal.&Prilozh. **25** (1991) 50; *Intersection Theory on the Moduli Space of Curves and the Matrix Airy Function*, Comm. Math. Phys. **147** (1992) 1–23.
- [30] M. Kontsevich, *Vassiliev’s knot invariants*, Adv. Sov. Math. **16** (1993) 137–150.
- [31] A. Loria, and T. Pan, *Domain structure of the ribozyme from eubacterial ribonuclease*, RNA **2** (1996) 551–563.
- [32] R. B. Lyngsø, and C. N. Pedersen, *RNA pseudoknot prediction in energy-based models*, J. Comput. Biol. **7** (2000) 409–427.
- [33] N. Marie, and K. Yeats, *A chord diagram expansion coming from some Dyson-Schwinger equations*, Comm. Numb. Theo. Phys. **7** (2013) 251–291, arXiv:1210.5457 [math.CO].
- [34] J. S. McCaskill, *The equilibrium partition function and base pair binding probabilities for RNA secondary structure*, Biopolymers **29** (1990) 1105–1119.
- [35] M. L. Mehta, *Random Matrices*, 2nd edition, Academic Press (1991).
- [36] A. Morozov, and Sh. Shakirov, *Generation of Matrix Models by \widehat{W} -operators*, JHEP **0904** (2009) 064, arXiv:0902.2627 [hep-th].
- [37] M. Mulase, *Lectures on the Asymptotic Expansion of a Hermitian Matrix Integral*, Springer Lecture Notes in Physics vol. 502, H. Aratyn et al., Editors, (1998) 91–134, arXiv:math-ph/9811023.
- [38] M. Mulase and P. Sulkowski, *Spectral curves and the Schroedinger equations for the Eynard-Orantin recursion*, Adv. Theor. Math. Phys. **19** (2015) 955–1015, arXiv:1210.3006 [math-ph].
- [39] M. Mulase, and A. Waldron, *Duality of Orthogonal and Symplectic Matrix Integrals and Quaternionic Feynman Graphs*, Commun. Math. Phys. **240** (2003) 553–586, arXiv:math-ph/0206011.
- [40] R. Nussinov, G. Piecchnik, J. R. Griggs, and D. J. Kleitman, *Algorithms for loop matching*, SIAM J. Appl. Math. **35** (1978) 68–82.
- [41] H. Orland, and A. Zee, *RNA Folding and Large N Matrix Theory*, Nucl. Phys. **B620** (2002) 456–476, arXiv:cond-mat/0106359 [cond-mat.stat-mech].
- [42] R. C. Penner, *The decorated Teichmüller space of punctured surfaces*, Comm. Math. Phys. **113** (1987) 299–339.
- [43] R. C. Penner, *Perturbative series and the moduli space of Riemann surfaces*, J. Diff. Geom. **27** (1988) 35–53.
- [44] R. C. Penner, *The simplicial compactification of Riemann’s moduli space*, Proceedings of the 37th Taniguchi Symposium, World Scientific (1996), 237–252.

- [45] R. C. Penner, *Cell decomposition and compactification of Riemann's moduli space in decorated Teichmüller theory*, In Tongring, N. and Penner, R.C. (eds) Woods Hole Mathematics-Perspectives in Math and Physics, World Scientific, Singapore, arXiv:math/0306190 [math.GT].
- [46] R. C. Penner, *Moduli spaces and macromolecules*, Bull. Amer. Math. Soc. (2016).
- [47] R. C. Penner, and M. S. Waterman, *Spaces of RNA secondary structures*, Adv. Math. **101** (1993) 31–49.
- [48] M. Peskin, and D. V. Schroeder, *An Introduction To Quantum Field Theory*, Westview Press (1995).
- [49] C. M. Reidys, *Combinatorial and computational biology of pseudoknot RNA*, Springer, Applied Math series 2010.
- [50] C. M. Reidys, F. W. D. Huang, J. E. Andersen, R. C. Penner, P. F. Stadler, and M. E. Nebel, *Topology and prediction of RNA pseudoknots*, Bioinformatics **27** (2011) 1076–85.
- [51] E. Rivas, and S. R. Eddy, *A dynamic programming algorithm for RNA structure prediction including pseudoknots*, J Mol Biol. **285** (1999) 2053–2068.
- [52] P. G. Silvestrov, *Summing graphs for random band matrices*, Phys. Rev. **E55** (1997), 6419.
- [53] D. W. Staple, and S. E. Butcher, *Pseudoknots: RNA structures with diverse functions*, PLoS Biol **3** (6) (2005) 956–959.
- [54] J. J. M. Verbaarschot, H. A. Weidenmuller, and M. R. Zirnbauer, *Grassmann integration in stochastic quantum physics: The case of compound nucleus scattering*, Phys. Rept. **129** (1985) 367–438.
- [55] G. Vernizzi, and H. Orland, *Large- N Random Matrices for RNA Folding*, Acta Phys. Polon. **B36** (2005) 2821–2827.
- [56] G. Vernizzi, H. Orland, and A. Zee, *Enumeration of RNA structures by Matrix Models*, Phys. Rev. Lett. **94** 168103, arXiv:q-bio/0411004 [q-bio.BM].
- [57] M. S. Waterman, *Secondary structure of single-stranded nucleic acids*, Adv. Math. (Suppl. Studies) **1** (1978) 167–212.
- [58] M. S. Waterman, and T. F. Smith, *RNA secondary structure: A complete mathematical analysis*, Math. Biosci., **42** (1978) 257–266.
- [59] E. Westhof, and L. Jaeger *RNA pseudoknots*, Curr. Opin. Chem. Biol. **2** (1992) 327–333.
- [60] M. Zucker, *On finding all suboptimal foldings of an RNA molecule*, Science **244** (1989) 48–52.
- [61] M. Zucker, and P. Stiegler, *Optimal computer folding of larger RNA sequences using thermodynamics and auxiliary information*, Nucleic Acids Res. **9** (1981) 133–148.

QGM, DEPARTMENT OF MATHEMATICS, AARHUS UNIVERSITY, DK-8000 AARHUS C, DENMARK
E-mail address: jea.qgm@gmail.com

FACULTY OF EDUCATION, KAGAWA UNIVERSITY, TAKAMATSU 760-8522, JAPAN
E-mail address: fuji@ed.kagawa-u.ac.jp

FACULTY OF PHYSICS, UNIVERSITY OF WARSAW, UL. PASTEURA 5, 02-093 WARSAW, POLAND
E-mail address: masahidemanabe@gmail.com

INSTITUT DES HAUTES ÉTUDES SCIENTIFIQUES, 35 ROUTE DE CHARTRES, 91440 BURS-SUR-YVETTE, FRANCE; DIVISION OF PHYSICS, MATHEMATICS AND ASTRONOMY, CALIFORNIA INSTITUTE OF TECHNOLOGY, PASADENA, CA 91125, USA
E-mail address: rpenner@caltech.edu, rpenner@ihes.fr

FACULTY OF PHYSICS, UNIVERSITY OF WARSAW, UL. PASTEURA 5, 02-093 WARSAW, POLAND; WALTER BURKE INSTITUTE FOR THEORETICAL PHYSICS, CALIFORNIA INSTITUTE OF TECHNOLOGY, PASADENA, CA 91125, USA
E-mail address: psulkows@fuw.edu.pl